

The University of Southern Mississippi
The Aquila Digital Community

Dissertations

Fall 12-2009

Remote Sensing of Harmful Algal Blooms in the Mississippi Sound and Mobile Bay: Modelling and Algorithm Formation

Dan Martin Holiday
University of Southern Mississippi

Follow this and additional works at: <https://aquila.usm.edu/dissertations>

 Part of the [Biology Commons](#), [Marine Biology Commons](#), and the [Plant Sciences Commons](#)

Recommended Citation

Holiday, Dan Martin, "Remote Sensing of Harmful Algal Blooms in the Mississippi Sound and Mobile Bay: Modelling and Algorithm Formation" (2009). *Dissertations*. 1085.
<https://aquila.usm.edu/dissertations/1085>

This Dissertation is brought to you for free and open access by The Aquila Digital Community. It has been accepted for inclusion in Dissertations by an authorized administrator of The Aquila Digital Community. For more information, please contact Joshua.Cromwell@usm.edu.

The University of Southern Mississippi

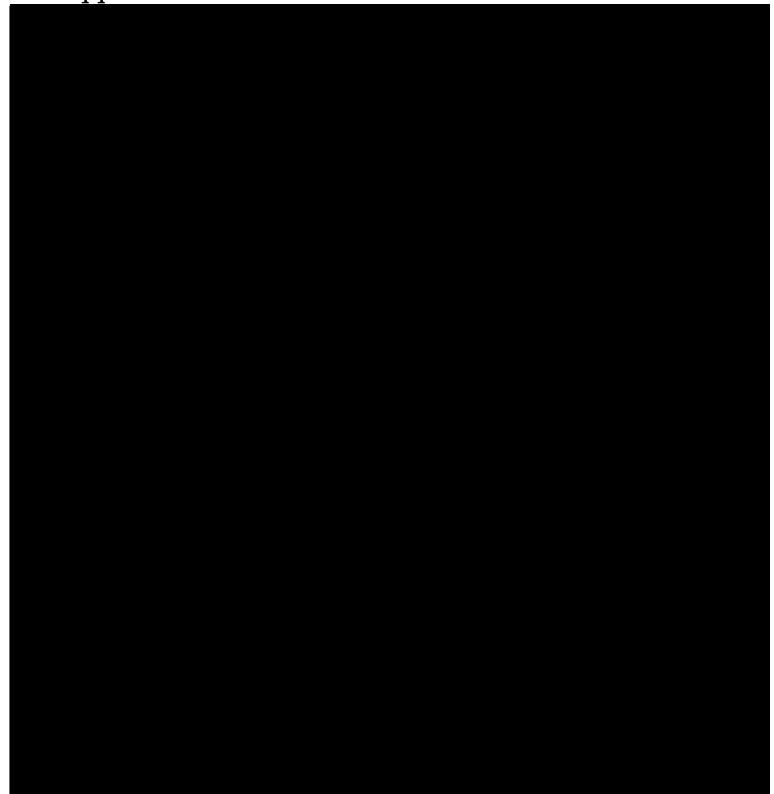
REMOTE SENSING OF HARMFUL ALGAL BLOOMS IN THE MISSISSIPPI
SOUND AND MOBILE BAY: MODELLING AND ALGORITHM FORMATION

by

Dan Martin Holiday

A Dissertation
Submitted to the Graduate School
of The University of Southern Mississippi
in Partial Fulfillment of the Requirements
for the Degree of Doctor of Philosophy

Approved:



December 2009

COPYRIGHT BY
DAN MARTIN HOLIDAY
2009

The University of Southern Mississippi

REMOTE SENSING OF HARMFUL ALGAL BLOOMS IN THE MISSISSIPPI
SOUND AND MOBILE BAY: MODELLING AND ALGORITHM FORMATION

by

Dan Martin Holiday

Abstract of a Dissertation
Submitted to the Graduate School
of The University of Southern Mississippi
in Partial Fulfillment of the Requirements
for the Degree of Doctoral Philosophy

December 2009

ABSTRACT

REMOTE SENSING OF HARMFUL ALGAL BLOOMS IN THE MISSISSIPPI SOUND AND MOBILE BAY: MODELLING AND ALGORITHM FORMATION

by Dan Martin Holiday

December 2009

The incidence and severity of harmful algal blooms have increased in recent decades, as have the economic effects of their occurrence. The diatom *Pseudo-nitzschia* spp. caused fisheries closures in Mobile Bay during 2005 due to elevated levels of domoic acid. In the previous 4 years *Karenia brevis* counts of $>5,000$ cells L^{-1} have occurred in Mobile Bay and the Mississippi Sound. Population levels of this magnitude had previously been recorded only in 1996. Increases in human populations, urban sprawl, development of shoreline properties, sewage effluent and resultant changes in N-P ratios of discharge waters, and decline in forest and marsh lands, will potentially increase future harmful algal bloom occurrences in the northern Gulf of Mexico.

Due to this trend in occurrence of harmful algal populations, there has been an increasing awareness of the need for development of monitoring systems in this region. Traditional methods of sampling have proven costly in terms of time and resources, and increasing attention has been turned toward use of satellite data in phytoplankton monitoring and prediction.

This study shows that remote sensing does have utility in monitoring and predicting locations of phytoplankton blooms in this region. It has described the composition and spatial and temporal relationships of these populations, inferring salinity, total nitrogen and total phosphorous as the primary variables driving

phytoplankton populations in Mobile Bay and the Mississippi Sound. Diatoms, chlorophytes, cryptophytes, and dinoflagellates were most abundant in collections. Correlations between SeaWiFS, MODIS and in situ data have shown relationships between R_{rs} reflectance and phytoplankton populations. These data were used in formation of a decision tree model predicting environmental conditions conducive to the formation of phytoplankton blooms that is driven completely by satellite data. Empirical algorithms were developed for prediction of salinity, based on R_{rs} ratios of 510 nm/ 555 nm, creating a new data product for use in harmful algal bloom prediction. The capacity of satellite data for rapid, synoptic coverage shows great promise in supplementing future efforts to monitor and predict harmful algal bloom events in the increasingly eutrophic waters of Mobile Bay and the Mississippi Sound.

ACKNOWLEDGEMENTS

I would like to thank my committee members, William Hawkins, Greg Carter, Patrick Biber, and Hugh Macintyre, for their patience and aid throughout the last three years. Also, I would like to thank Bill Smith and Carol Dorsey of the Alabama Department of Public Health for their expertise in identifying the phytoplankton within samples collected during research for this work, members of the Dauphin Island MacIntyre lab for their scientific and moral support, and thank David Burke just for being David Burke during the hours we spent on the boat while collecting those samples.

My appreciation is extended to Dr. Carlos Del Castillo of the Johns Hopkins Applied Physics Institute for his suggestions and contributions toward the formation of the empirical algorithms, and Rick Gould and Rebecca Green of the Naval Research Laboratory at Stennis Space Center for their aid in acquiring and in creating an opportunity to learn methods of analyzing SeaWiFS and MODIS imagery.

Most importantly, thank you Ann and Sylva, and my Mother and Father.

This research was supported in part by EPA Grant MX964236-05-0 “Remote Sensing of Harmful Algal Blooms in Mobile Bay and the Mississippi Sound”, the Northern Gulf Institute, and the NASA Graduate Student Researchers Fellowship.

TABLE OF CONTENTS

ABSTRACT	ii
ACKNOWLEDGMENTS.....	iv
LIST OF TABLES.....	vii
LIST OF ILLUSTRATIONS.....	viii
CHAPTER	
I. INTRODUCTION.....	1
II. FACTORS AFFECTING THE SPATIAL AND TEMPORAL DISTRIBUTIONS OF PHYTOPLANKTON POPULATIONS IN MOBILE BAY AND THE MISSISSIPPI SOUND OF THE NORTHERN GULF OF MEXICO.....	7
Introduction	
Methods	
Results	
Conclusions	
III. THE USE OF SEAWIFS DATA IN FORMING DECISION TREE MODELS TO PREDICT BLOOMS OF PSEUDO-NITZSCHIA IN MOBILE BAY	27
Introduction	
Methods	
Results	
Discussion	
IV. THE USE OF IN SITU REMOTE REFLECTANCE DATA TO FORM REGIONAL ALGORITHMS FOR SALINITY AND CDOM PREDICTION	37
Introduction	
Methods	
Results	
Conclusions	
V. SUMMARY.....	49
APPENDIX.....	52

REFERENCES.....56

LIST OF TABLES

Table

1. Eigenvalues and eigenvectors from PCA analysis in Figure 5.....21
2. Station information, salinity and CDOM values. Note the inverse relationship between salinity and a_g41243

LIST OF ILLUSTRATIONS

Figure

1. Collection sites in Mobile Bay, Pass Aux Herons, and the Mississippi Sound. Symbols represent location of site collections, darker symbols represent higher numbers of collections at that collection location.....12
2. Horizontal dotted line representing a similarity threshold line was set at 50% for similarity within community groups of field collections. Clusters (classes) represented by the classes below the 50% similarity threshold line were used as factors in MDS and PCA analyses.....15
3. Multi-dimensional scaling plot (based on Bray-Curtis similarity matrices) of phytoplankton composition based on factors from Figure 2. Analysis was carried out using individual collections from all sites made during the 18 month period. Note the high degree of similarity, or close spatial relationship on the 2-dimensional ordination, between members of a class resulting in clustering of samples within classes i and k.....17
4. Pie graphs illustrating SIMPER analysis of the average abundance of taxa contributing to within site similarity. Data represented below class taxa is the average abundance within classes.....18
5. Relative abundance of diatom, chlorophytes, cryptophytes, and dinoflagellate collections. Charts show seasonal trends with diatom and dinophyte abundances higher in winter and spring, and chlorophytes and cryptophytes abundances higher in summer and fall months.....19
6. PCA analysis of S, T, pH, TN, TP, aD400, TSS, and MSS. Note the axes of the eigenvectors S, TN, and TP, and their orientation with the data classes i and k...20
7. Stack graph with 5 panels showing the relative influence of total combined mean monthly discharge ($m^3 s^{-1}$) from the Mobile and Tensaw Rivers on S (psu), TN ($\mu mol L^{-1}$), TP ($\mu mol L^{-1}$), and Chla ($\mu mol L^{-1}$) concentrations at the Mid-Bay Lighthouse.....23
8. The relationship between S and discharge at Mid-Bay Lighthouse and the east end of Dauphin Island. Discharge values are averages of 14 days before collection date. Note the inverse relationship between river discharge and salinity.....24

9.	Box plots of S, TN, and TP, from all collections at Mid-Bay Lighthouse. The lower, middle, and upper lines of the boxes represent the first quartile, median, and third quartile, respectively. The bars extending from the boxes represent data range, black diamonds represent data maximum and minimum.....	25
10.	Map of collection sites in Mobile Bay, AL, and the eastern Mississippi Sound. <i>Pseudo-nitzschia</i> spp. population data from sites marked in solid gray were used in DT formation and testing. Sites from this area of Mobile Bay and surrounding waters were used due to maximum values of population data and common presence of <i>Pseudo-nitzschia</i> spp. within collections.....	31
11.	Visualization of Decision Tree classifier from ENVI v4.3. Notice titles of nodes indicating factors used in formation of the statement for the node, while percentages within each leaf represent number of pixels affected by the statement. This output is a result of the test performed on figure 3.D., showing 0.91% of pixels (1,409 of 158,400) having the unique set of environmental properties enabling <i>Pseudo-nitzschia</i> spp. to be present in high population numbers.....	33
12.	SeaWiFS R_{rs} products at 555 and 670nm, and quotient of these wavelengths at 670/555, with <i>Pseudo-nitzschia</i> spp. (cells L^{-1}) represented on the y-axis, natural log scale applied to data for allowing observation of cell numbers $>10^4$ cells L^{-1} . Note the spread of data points $<10^4$ at all wavelengths, and narrowing of data range when a 670/555 nm ratio is applied to R_{rs} data.....	34
13.	A. SeaWiFS image from May 6, 2006, R_{rs} at 670 nm, 1 km resolution. Red dots indicate locations of in situ collections. B. Results from decision tree analysis, using <i>Pseudo-nitzschia</i> spp. counts from May 6, 2006. White dots indicate location of in situ data collections, spatial coverage is identical to Figure 3A. C. SeaWiFS image from April 4, 2005, R_{rs} at 670 nm, 1 km resolution. Red dots indicate locations of in situ collections. D. Results from decision tree analysis, using <i>Pseudo-nitzschia</i> spp. counts from April 4, 2005. White dots indicate location of in situ data collections, spatial coverage is identical to Figure 3C.....	35
14.	Locations of stations used in collection of water samples, in situ spectroradiometer readings, and SeaWiFS data extractions.....	41
15.	Absorption spectra of CDOM obtained from samples collected in the MS.....	45
16.	a_g 412 vs. salinity from samples collected in the Mississippi sound.....	45
17.	R_{rs} data collected from in situ stations in the MS.....	46

- 18. Comparison between field and remote sensing measurements of R_{rs} . Field and remote sensing images were collected on October 25 and 26, 2007. Linear equations developed using TableCurve v5. Note $R^2 = .87$ using MODIS data, and $R^2 = .89$ using SeaWiFS data. Spectroradiometer field data and corresponding R_{rs} sensor data show ranges of <0.025 l/sr.....46
- 19. Remote sensing retrievals of a_g412 and salinity based on empirical algorithms developed in this work. Images are based on SeaWiFS data collected on second collection day, and processed using SeaDAS v5.4.....48

CHAPTER I

INTRODUCTION

Harmful algal blooms (HABs) are proliferations of microalgae accumulating at biomass levels that negatively affect co-occurring organisms and the food web. Some harmful algae (HA) species produce phycotoxins that bioaccumulate in shellfish and fish. Others proliferate in response to changing environmental conditions, such as nutrient flux and eutrophication, creating hypoxic or anoxic conditions. A third type produces calciferous appendages that damage gill and digestive tissues of shell and finfish (Granéli & Turner, 2006; HAARNESS, 2005). Over the past several decades, the frequency and severity of HABs has increased in USA coastal areas (Anderson, Glibert, & Burkholder, 2002; HAARNESS, 2005). These blooms have caused regional economic losses at an estimated average of 82 million dollars annually in North America since 1987 (Hoagland & Scatasta, 2006) due to human health problems, loss of tourism, commercial and recreational fishing closures, ecosystem damage, and cleanup costs.

In Mobile Bay (MB) and the eastern Mississippi Sound (MS), surveys carried out by Pennock et al. in 2001 and 2002, the Gulf Coast Geospatial Center (GCGC) from July 2005 through June 2006, and routine surveys done by Dauphin Island Sea Lab (DISL) and the Alabama Department of Public Health (ADPH), regularly identified species of microalgae with the potential to create HAB events. To date, 7 known HA species have been detected at significant levels ($>10^5$ cells L⁻¹) in coastal waters of the northern Gulf of Mexico (GoM). These include the diatoms *Pseudo-nitzschia* spp. and the dinoflagellates *Karenia brevis*, *Gymnodinium sanguineum*, *Dinophysis caudata*, and *Prorocentrum minimum*. *Pseudo-nitzschia* produces domoic acid, the causative agent in amnesiac shellfish poisoning (ASP). *Karenia*, *Gymnodinium*, and *Dinophysis* produce

brevitoxin, saxitoxins, and okadaic acid, respectively, with these toxins being responsible for neurotoxic, paralytic, and diarrhetic shellfish poisoning (NSP, PSP, and DSP) (Landsberg, 2002). *Karlodinium veneficum*, a producer of karlotoxins, *Heterocapsa triquetra*, and *Akashiwo sanguinea*, two dinoflagellates found in high cell concentrations leading to hypoxic conditions, have caused fish kills in MB (Bill Smith, ADPH). Other potential HA species, such as the dinoflagellates *Karenia mikimotoi*, associated with massive fish kills in Japan and Korea, and two members of the genus *Gonyaulax*, *G. spinifera* and *G. polygramma*, both associated with red tides in Florida (Landsberg, 2002; Steidinger & Penta, 1999), have been found at low levels (<2000 cells L⁻¹).

Two of these HAB-related organisms are of greatest concern in this region, the dinoflagellate *K. brevis* and diatoms of the genus *Pseudo-nitzschia*. *K. brevis* releases brevetoxins, causing respiratory damage and NSP in human populations while creating adverse affects on ecosystems and food webs, including strandings and death to dolphins, fish kills, closures of shell and finfish operations and subsequent economic losses due to halo effects of these events through coastal and regional populations (Steidinger & Penta, 1999; Steidinger, Landsberg, Truby, & Roberts, 1998). The only known *K. brevis* bloom resulting in closed shellfish operations in coastal Mississippi and Alabama occurred in 1996 (Dortch et al., 1997). Historically, *K. brevis* blooms have been documented since the Spanish explorers first arrived in the GOM during the 17th century (Magaña, Contreras, & Villareal, 2003). In the preceding few decades blooms have occurred bi-annually or less off the western coast of Florida and coasts of Texas and eastern Mexico (Steidinger et al., 1998; Tomlinson et al., 2004; Villareal, Brainard, & McEachron, 2001). However, *K. brevis* blooms have increased in frequency, duration, and intensity in these

locations and programs are in place for monitoring and predicting these occurrences (Stumpf et al., 2009; Tomlinson et al., 2004). In MB and surrounding waters, *K. brevis* has been detected in samples at cell counts of $>5,000$ cells L^{-1} in 2005, 2006, and 2007 (personal communications, Hugh MacIntyre, DISL, and Bill Smith, ADPH). Mechanisms of bloom formation are not yet conclusive but hypotheses include elevated nutrient runoff resulting from anthropogenic influences related to increased coastal development and human population growth, ecosystem damage, fluctuation in salinity or nutrient concentrations and ratios, ocean wave propagation and turbulence due to physical forcing and storm events, prevailing winds and currents driving blooms from Florida shores, atmospheric input of Sahara dust, and bacterial interactions (Burkholder et al., 2007; Cortes-Altamirano, Hernandez-Becerril, & Luna-Soria, 1995; Jewett, Dortch, & Etheridge, 2007; Kin-Chung & Hodgkiss, 1991; Maier Brown et al., 2006; Smayda, 1997; Sommer, 1994).

There are approximately 50 species of the diatom genus *Pseudo-nitzschia* found world-wide (Bates & Trainer, 2006). Domoic acid, the phycotoxin responsible for ASP, is known to be produced by 11 of them. Seven of these toxin-producing species have been found in samples from the northern GoM, sometimes in excess of 10^6 cells L^{-1} (Liefer et al., 2009; Thessen, Dortch, Parsons, & Morrison, 2005). These are euryhaline organisms, rarely found more than 150 km from shore. They are abundant in coastal environments where wide ranges of salinity, temperature, and turbidity are found (Bates & Trainer, 2006; Dortch et al., 1997; Hasle, 2002). Domoic acid poisoning has been found to be a common cause of die-offs in mammals, birds, turtles, and fish on the northeast and southwest coasts of North America (Bates, Garrison, & Horner, 1998;

Landsberg, 2002), and ASP was shown to be the cause of 5 human deaths in eastern Canada in 1987 (Bates et al., 1989). To date, no marine animal die-offs or human cases of ASP have been attributed to domoic acid poisoning in the northern GOM. This is due possibly to genetic variation and the presence of low or non-toxic strains, and the fact that most samples containing high counts of *Pseudo-nitzschia* spp. and detectable domoic acid levels are collected in slightly deeper and more mixed waters away from harvested oyster beds (Thessen et al., 2005). However, the fact that these species thrive in the northern GOM, combined with expectations of rising nutrient levels driven by increases in human population and changes in land use patterns, makes them a potential threat to human and ecosystem health.

Mitigation of regional problems caused by HAB outbreaks requires a combination of monitoring the presence of HAB species and the conditions leading to or indicative of their formation, prediction of ecological conditions allowing their formation, prediction of the size and movement patterns of known blooms, and subsequent response and control efforts (HAARNESS, 2005; Stumpf et al., 2009). Monitoring of HAB species is costly in equipment purchase and ship and shore collection expenditures. Arguably most important is the investment of time. This includes both time spent in planning, carrying out, and processing sample collections and the subsequent delay in response time due to these efforts. For these reasons, there is great interest in the use of remote sensing to detect HAB and predict migration patterns of known blooms (Siegel, Maritorena, Nelson, Behrenfeld, & McClain, 2005; Stumpf et al., 2003). The use of satellite sensors such as the Sea-viewing Wide Field-of-view Sensor (SeaWiFS) and the MODerate-resolution Imaging Spectroradiometer (MODIS) enables twice-daily (MODIS Aqua PM and

SeaWiFS noon), wide-area coverage not economically or temporally possible with traditional ship and shore survey techniques (Tatem, Goetz, & Hay, 2004).

This research is directed toward understanding the factors driving the spatial and temporal composition of phytoplankton populations in this region while evaluating and utilizing remote sensing data for development of a predictive model based on these factors. The following research objectives will be explained in Chapters II-IV:

Chapter II: Factors affecting the spatial and temporal distributions of phytoplankton populations in Mobile Bay and the Mississippi Sound of the Northern Gulf of Mexico

The objectives of this chapter are to 1) describe the composition of phytoplankton populations at collection sites in Mobile Bay and the eastern Mississippi Sound, 2) determine what relationships exist within and between those populations, 3) describe the environmental variables most significant in driving these relationships, and 4) illustrate seasonality of these populations, and influence of river discharge on significant environmental variables.

*Chapter III: Development of a decision tree model for *Pseudo-nitzschia* spp*

The purpose of this chapter is to utilize SeaWiFS remote sensing reflectance data in the formation of a decision tree model that will allow for the prediction of ecological conditions most suitable for development of *Pseudo-nitzschia* spp. blooms. Primary objectives are to 1) determine correlations between in situ and remote sensing data and utilize SeaWiFS data most suitable for use in a decision tree model, and 2) create and test the model using *Pseudo-nitzschia* spp. population and remote sensing data.

Chapter IV: Using in situ spectroradiometer data to develop a regional specific algorithm for prediction of salinity in the waters of MB and MS

The goal of this chapter is to develop regional-specific algorithms for predicting salinity in the MS based on in situ CDOM measurements. Primary objectives of this chapter are to 1) use in situ surface reflectance values measured during cruises undertaken in the MS to emulate the SeaWiFS remote sensing reflectance values (R_{rs}) at 412, 443, 490, 510, 555, and 670 nm, 2) compare these emulated R_{rs} values with SeaWiFS and MODIS R_{rs} values obtained from same day imagery, and 3) develop and test a region-specific empirical algorithm for salinity.

CHAPTER II
FACTORS AFFECTING THE SPATIAL AND TEMPORAL DISTRIBUTIONS OF
PHYTOPLANKTON POPULATIONS IN MOBILE BAY AND THE MISSISSIPPI
SOUND OF THE NORTHERN GULF OF MEXICO

Introduction

Understanding the organization of phytoplankton populations is based upon attempts to reveal recurring patterns and variations that occur through space and time as explainable phenomena (Levin, 1992). The detection and description of recurring patterns that cannot be attributed to chance provide a logically constructed framework used to infer causes and comprehend underlying mechanisms of the synergistic relationships between biotic and environmental data (Field, Clarke, & Warwick, 1982).

The majority of studies concerning driving forces behind abundance and diversity of phytoplankton populations in near-shore and estuarine environments have focused on temperate ecosystems in well-studied estuaries such as Chesapeake Bay (Marshall, Lacouture, & Johnson 2006; Harding et al., 1994), San Francisco Bay (Lucas, Koseff, Cloern, Monismith, & Thompson 1999a, 1999b) and Pamlico Sound (Gallegos & Platt, 1982; Lohrenz, Redalje, Verity, Flagg, & Matulewski, 2002). In recent years attention has been given to biological, physical and chemical gradients driving phytoplankton population dynamics within sub-tropical blackwater river systems of Florida (Bledsoe & Phlips, 2000; Quinlan & Phlips, 2007). The majority of these studies have concentrated on estuaries and bays with water residence times in month to year temporal cycles (Phlips, Badylak, Youn, & Kelley, 2004; Harding, Itsweire, & Esaias, 1994), systems that are influenced primarily by strong tidal regimes (Lucas et al., 1999a; Cloern, 1991), or

seasonal upwelling caused by wind and current interactions (Anderson et al., 2008; Lanerolle et al., 2006). Recent studies have demonstrated the importance of salinity gradients and their effects on spatial patterns of available nutrients and distribution of phytoplankton populations in estuaries (Quinlan & Phlips, 2007; Muylaert, Sabbe, & Vyverman, 2009).

This study focuses on Mobile Bay (MB) and the eastern Mississippi Sound (MS) in the northern Gulf of Mexico. These systems are dominated by freshwater discharge (Schroeder, 1977; Wilber, Clarke, & Rees, 2007) and short residence times of hours to days (Schroeder, 1979). Past work within MB has suggested a coupling between watershed basin discharge, residence time and nutrient fluxes (Lehrter, 2008) and a coupling of benthic and pelagic processes (Cowen, Pennock, & Boynton, 1996) leading to spatial variability of nutrients. Neither the taxonomy of the microalgal populations of these systems nor the factors which drive their abundance, composition or distribution have been well described. Pennock et al. (2001, 2002) conducted cruises which described phytoplankton populations within MB and its major sub-estuary, Weeks Bay. They found that MB was similar to most shallow estuary systems dominated by freshwater input, in that there is a nutrient pulse associated with late winter and spring rains, but there was no well-developed spring bloom associated with this input. Liefer et al. (2009) described the occurrence and distribution of *Pseudo-nitzschia spp.* in the southern reaches near the mouth of MB. This toxin-producing harmful algal bloom diatom was found to be a common member of microalgal communities throughout the Mississippi Bight. Its presence within samples was reported over a wide range of salinity and surface temperature ranges. They found samples at high numbers correlated to salinity levels and

influenced by nutrients from freshwater input, primarily groundwater discharge.

The objectives of this paper are to describe the spatial and temporal variability of phytoplankton populations and their relationships with environmental data in this region. The data set used in describing these relationships consisted of sampling stations ranging spatially from the north end of MB to Horn Island and Biloxi Bay in the eastern MS (Fig. 1), and temporally over an 18 month period from 12/2004 – 6/2006. It is shown that salinity, total nitrogen, and total phosphorous are the most significant factors driving phytoplankton populations in this region. It is inferred that the combined Mobile-Tensaw and Biloxi-Pascagoula River discharge influences abiotic variables, which in turn influence the composition of phytoplankton populations. Seasonal patterns are shown to exist, with diatoms and dinoflagellates exhibiting population peaks in the winter and spring months, and chlorophytes and cryptophytes in the summer and fall months.

Site Description

The MB estuary (30.5 N, 88.0 W) is a drowned river system, approximately 50 km long with a width of up to 31 km (Schroeder, 1977). It is a shallow (average depth 3m), highly stratified estuary with a surface area of approximately 1,070 km², a relatively small volume of 3.2×10^9 m³ and a short residence time of days to weeks (Engle, Kurtz, Smith, Chancy, & Bourgeois, 2007). A dredged shipping channel runs north to south from the city of Mobile through Main Pass to the east of Dauphin Island, creating maximum depth waters of 15 m (Isphording & Lamb, 1979). Disposal of dredged materials in open water adjacent to the channel has influenced bottom contours, particularly at the northern bay and west of the channel where spoil banks influence water circulation and stratification of the water column (Schroeder, Cowan, Pennock, Luker, &

Wiseman, 1998). River discharge and seasonal wind patterns rather than tidal cycles control the hydrology of the estuary, with water quality being heavily influenced by groundwater input, regional weather patterns, dredging and subsequent deposition of tailings and human land use patterns throughout the watersheds of the estuary (Engle et al., 2007; Schroeder et al., 1998; Turner, Schroeder, & Wiseman, 1987). The mouth of MB is formed by Cedar Point to the west and Ft. Morgan Peninsula to the east. At the north end, the Mobile River is formed by the confluence of the Alabama and Tombigbee Rivers, combining to form the fourth largest watershed in the coterminous United States (Bricker et al., 2007). This system dominates water flow into the bay, contributing 95% of freshwater input (Schroeder et al., 1979). The addition of freshwater from the Dog and Fowl Rivers on the west shore and Fish and Magnolia Rivers flowing into Weeks Bay along the east shore create a short freshwater fill time of approximately 20 days (Cowan, Pennock, & Boynton, 1996), and an average daily freshwater flow of $1.56 \times 10^8 \text{ m}^3 \text{ d}^{-1}$ (Engle et al., 2007). This creates an average monthly discharge rate into the northern GoM of $1,800 \text{ m}^3 \text{ s}^{-1}$ (for the period from 1929 to 1983, see Schroeder & Wiseman, 1986). The land mass of Dauphin Island channels discharge flow, with approximately 15% passing to the north and west of the island through the east end of MS by way of Pass Aux Heron and the remainder, including contributions from the shipping channel, flow south and west through the main pass between the island and Ft. Morgan Peninsula (Ryan et al., 1997; Schroeder et al., 1992). These various contributions combine to create a highly stratified, rapidly changing environment (Schroeder, Dinnel, & Wiseman, 1990; Noble, Schroeder, Wiseman, Ryan, & Gelfenbaum, 1996).

The MS (30.2 N, 88.3W) is a shallow coastal lagoon with a mean depth of 3 m,

approximately 130 km long and 11-24 km wide, bordered on the south by a series of barrier islands and on the north by the mainland shoreline of Mississippi (Wilber et al., 2007). The combination of shipping channels (Gulf Intracoastal Waterway and the Biloxi Shipping Channel) running east to west and into Biloxi Bay and the coastal littoral current brings MB discharge waters from both Pass Aux Heron and the main pass of MB between Dauphin Island and Fort Morgan Peninsula into the MS, where they mix with fresh water outputs of the Pascagoula, Biloxi, and several smaller river systems (Rabalais, Dagg, & Boesch, 1985; Dinnel & Schroeder, 1989). Waters from the MS are generally well-mixed with minimal difference between surface and bottom temperature and salinity (Wilber et al., 2007).

Methods

In Situ Sampling

Surface water samples were collected at 3-6 week intervals from December, 2004, through June, 2006, at 19 sites in Mobile Bay (N= 197) and from July, 2005 through June, 2006 at 5 sites in the Mississippi Sound (N= 50) that encompass the major hydrological regimes in Mobile Bay and its adjacent waters in the Mississippi Sound (Fig. 1). An additional 25 sites were utilized throughout the collection period. The Mobile Bay sites are situated at principle inflows (stations near mouths of Mobile River, Dog River, Fowl River, and Weeks Bay), outflows (Pass Aux Herons and Main Pass), over oyster beds near Cedar Point and within Bon Secour Bay and at sites located near Dauphin Island and Ft. Morgan Peninsula. Sites in the Mississippi Sound follow a south transect from the mouth of Biloxi Bay through Dog Keys Pass and between Horn and Ship Islands. One exception was off the northeast shore of Horn Island, a site within the

MS ship channel and away from the influence of the Biloxi Bay discharge. No samples were collected in the MS during September and October of 2005 due to environmental and infrastructure damage caused by Hurricanes Katrina and Rita.

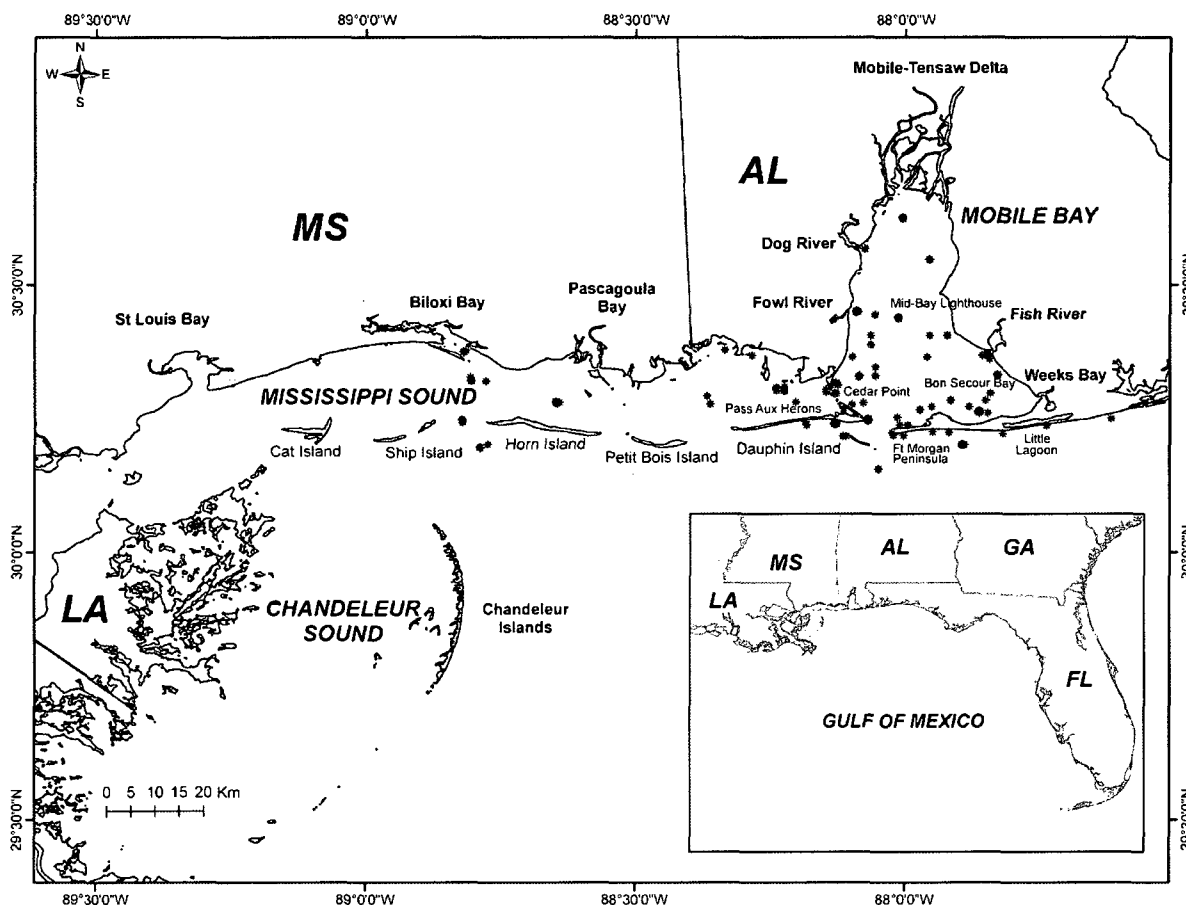


Figure 1. Collection sites in Mobile Bay, Pass Aux Herons, and the Mississippi Sound. Symbols represent location of site collections, darker symbols represent higher numbers of collections at that collection location.

Laboratory Analysis

In the laboratory, nutrient water samples were filtered through GF/F glass filters (0.7 μ m pore size) separating water sample into particulate phase collected on the filter and dissolved constituents in the filtrate. Physical parameters (T, S, pH) were measured at each sampling site using a hand held YSI. Unique surface water samples were taken for analysis of nutrient pool sizes and microalgal abundances. For all sampling trips, water samples were kept on ice in the dark until processing in the laboratory.

Chlorophyll *a* (Chl*a*) was measured fluorometrically on a Turner Designs fluorometer (TD 700) and recorded in μ g L⁻¹. Inorganic nutrients (NO₃⁻, NO₂⁻, NH₄⁺, and PO₄⁻³) were determined directly by colorimetric techniques modified for the Skalar SAN+ nutrient autoanalyzer. Particulate organic phosphorus (POP), dissolved organic phosphorus (DOP), and total dissolved nitrogen (TDN) concentrations were also measured with the Skalar SAN+ autoanalyzer. Particulate carbon and nitrogen were measured on a Costech CNS analyzer. Dissolved inorganic carbon (DIC) and dissolved organic carbon (DOC) were determined using a Shimadzu TOC analyzer. Filter pads with suspended solids were dried at 60°C and muffled at 500°C. Total suspended solids (TSS) were determined as weight of dried particulates per volume filtered, mineral suspended solids (MSS) were determined as weight of muffled particulates per volume filtered, and organic suspended solids (OSS) were determined as the difference between dried and muffled weight per volume filtered.

Dissolved inorganic nitrogen (DIN) was calculated as the sum of NO₃⁻, NO₂⁻, and NH₄⁺. Dissolved organic nitrogen (DON) was calculated as the difference between TDN

and DIN. Total nitrogen (TN), total phosphorus (TP), and total carbon (TC) are the sum of dissolved and particulate pools, recorded in $\mu\text{ mol L}^{-1}$.

Unique samples were collected from the surface waters for both phytoplankton and nutrient sample collection. One liter of whole water was preserved immediately upon collection with Lugol's solution. Phytoplankton cell counts were determined by the Alabama Department of Public Health (ADPH) using inverted light microscopy. Class level cell counts were used in analysis. Diatoms (bacillariophytes, fragilariophytes, coscinodiscophytes), dinoflagellates, chlorophytes, prasinophytes, euglenophytes, cryptophytes, dictyophytes, chrysophytes, and raphidophytes were enumerated in a settling Nunc chamber and counted at cells L^{-1} . Colonies rather than individuals of cyanobacteria were counted, and therefore not included in the analysis due to potential statistical anomalies introduced by this disparity in counting method.

Statistical Analysis

Phytoplankton community composition was analyzed using statistical software Primer-E v6. Ordination methods of multidimensional scaling (MDS) and principle components analysis (PCA) were used to examine spatial patterns of phytoplankton community compositions and influence of nutrient fluxes on abundances, based on analytical methods described by Clarke and Warwicke (2001). Environmental variables used in analysis were determined using draftsman plots to visualize relationships between variables, and were $\log(x+1)$ transformed if necessary and normalized. Cluster analysis of class level data from collections (N=247) was performed (Fig. 2). A 50% threshold similarity line was chosen, resulting in groupings of 7 major (≥ 5 collections within a

cluster) and 8 minor clusters, or classes (<5 collections within a cluster). These class groupings were used as factors to illustrate community composition patterns using MDS, plotting the dissimilarity of class groupings within Euclidean space. PCA was used for analysis of environmental variables influences on community structure, again using the

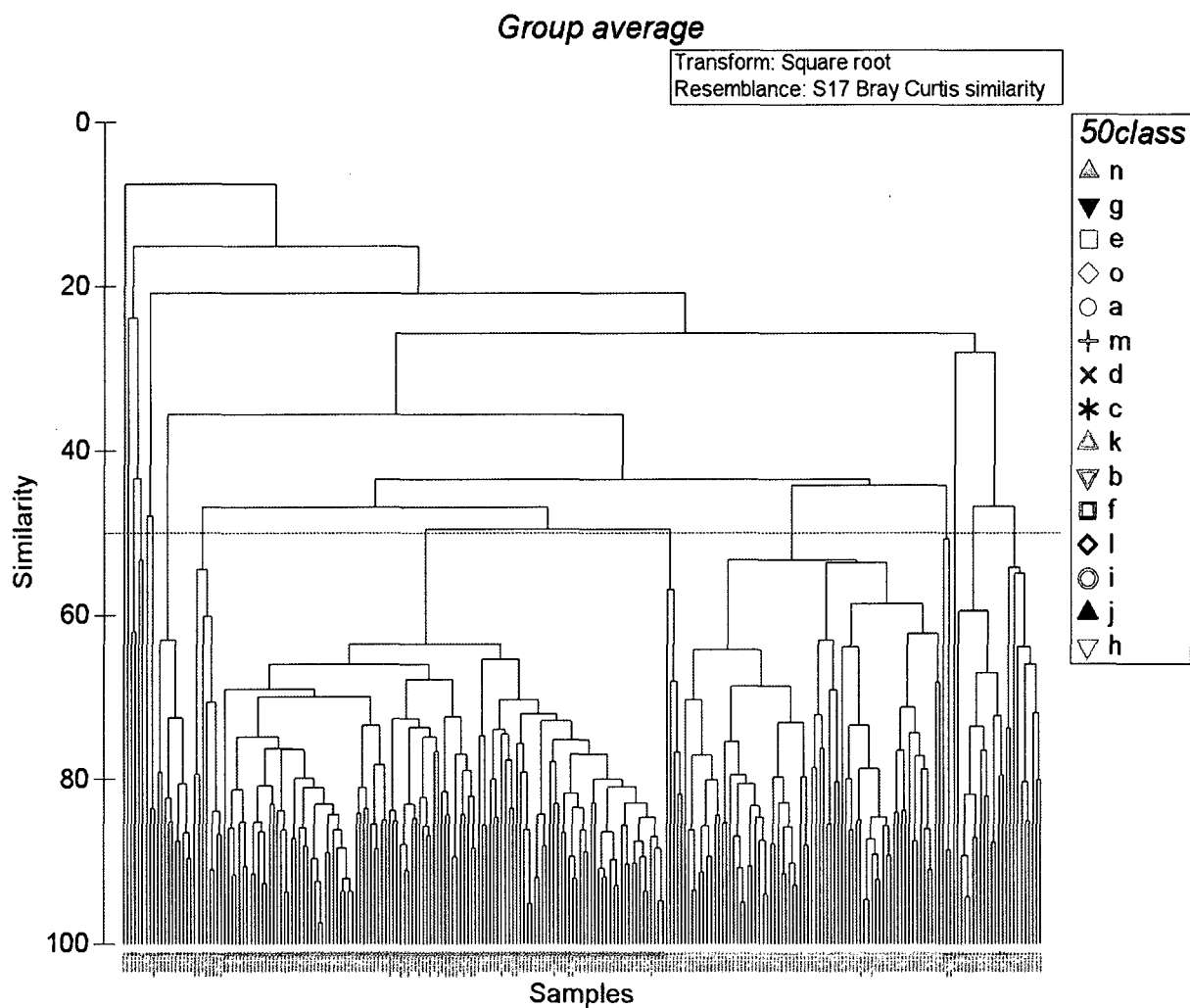


Figure 2. Horizontal dotted line representing a similarity threshold line was set at 50% for similarity within community groups of field collections. Clusters (classes) represented by the classes below the 50% similarity threshold line were used as factors in MDS and PCA analyses.

classes as factors within analysis. Similarity of percentage (SIMPER) analysis examine contribution of taxa within each class to similarities within class assemblages. The more abundant a taxon is within a group, the more it contributes to intra-group similarities. Information on the structure of abundance is summarized by Bray-Curtis similarities between samples (i. e. classes) and it is by computing the average dissimilarity between all pairs of inter-class samples (e.g. all collections within class i compared to all collections within class k, and so on), then using these data to perform similar averaging to understand the similarities, or the contributions of each taxon within the classes. These abundances are illustrated through pie charts demonstrating the contribution (or average abundance) of each taxon to the composition of the phytoplankton populations within classes, and the average similarity of taxa within the classes.

Results

Phytoplankton Populations

Community composition using the classes from the 50% similarity threshold chosen in cluster analysis and used as factors within an MDS plot (Figure 3) resulted in strong similarities within phytoplankton communities. Although stress similarities were relatively high for this method of ordination (2D= .15, 3D= .11), the number of samples (N= 247), each representing class-level phytoplankton populations, and the close grouping of samples within the major classes (those consisting of ≥ 5 collections) illustrate the strength of the relationships (Clarke & Warwick, 2001; Clarke, 1993; Kruskal, 1964). Classes i (N= 118) and k (N= 69), the 2 clusters representing the highest number of collections during sampling, show close relationships within both the 2D and 3D graphs (3D not shown).

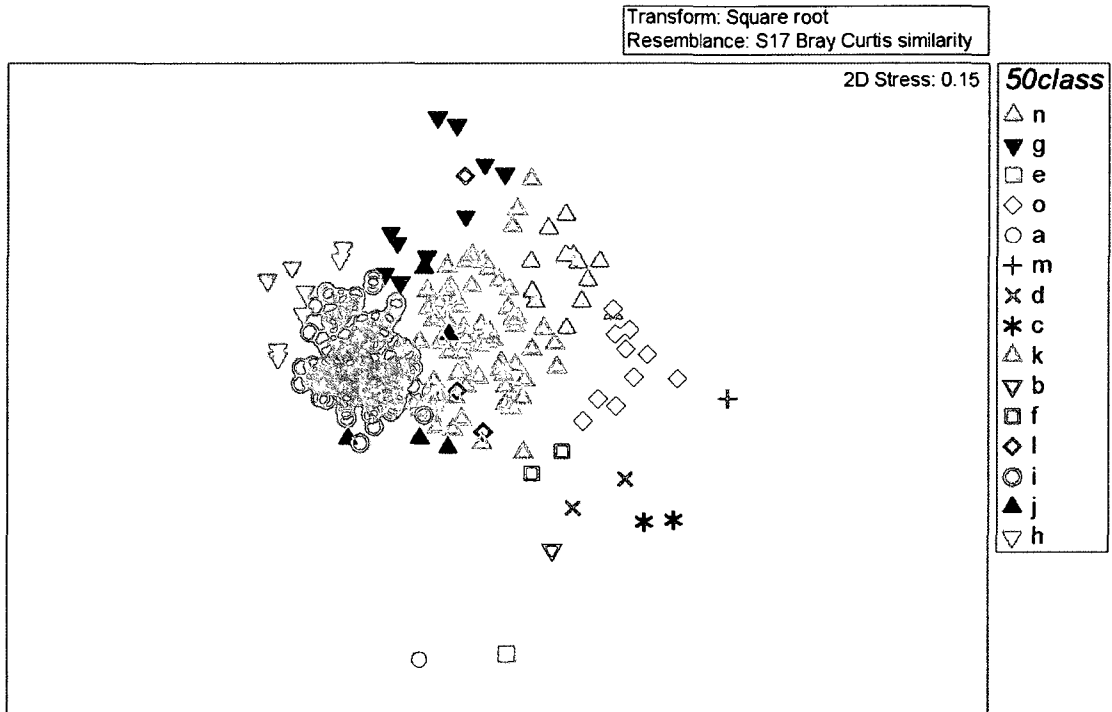


Figure 3. Multi-dimensional scaling plot (based on Bray-Curtis similarity matrices) of phytoplankton composition based on factors from Figure 2. Analysis was carried out using individual collections from all sites made during the 18 month period. Note the high degree of similarity, or close spatial relationship on the 2-dimensional ordination, between members of a class resulting in clustering of samples within classes i and k.

SIMPER analysis was used to determine which taxa were responsible for differences between and within classes. The influence of diatoms in the biomass of all sites (Fig. 4) was shown through their being absent as a significant component of collections in only one class (class h). Dinoflagellates comprised the majority of collections only in Class h, due to a February, 2006, *Heterocapsa triquetra* bloom in Mobile Bay. Chlorophytes were dominant in class i, comprising the majority of collections made during the mid- to late summer of 2005. Collections dates surrounded the passages of Hurricanes Katrina and Rita. Cryptophytes dominated in class j, consisting primarily of collections in November, 2005.

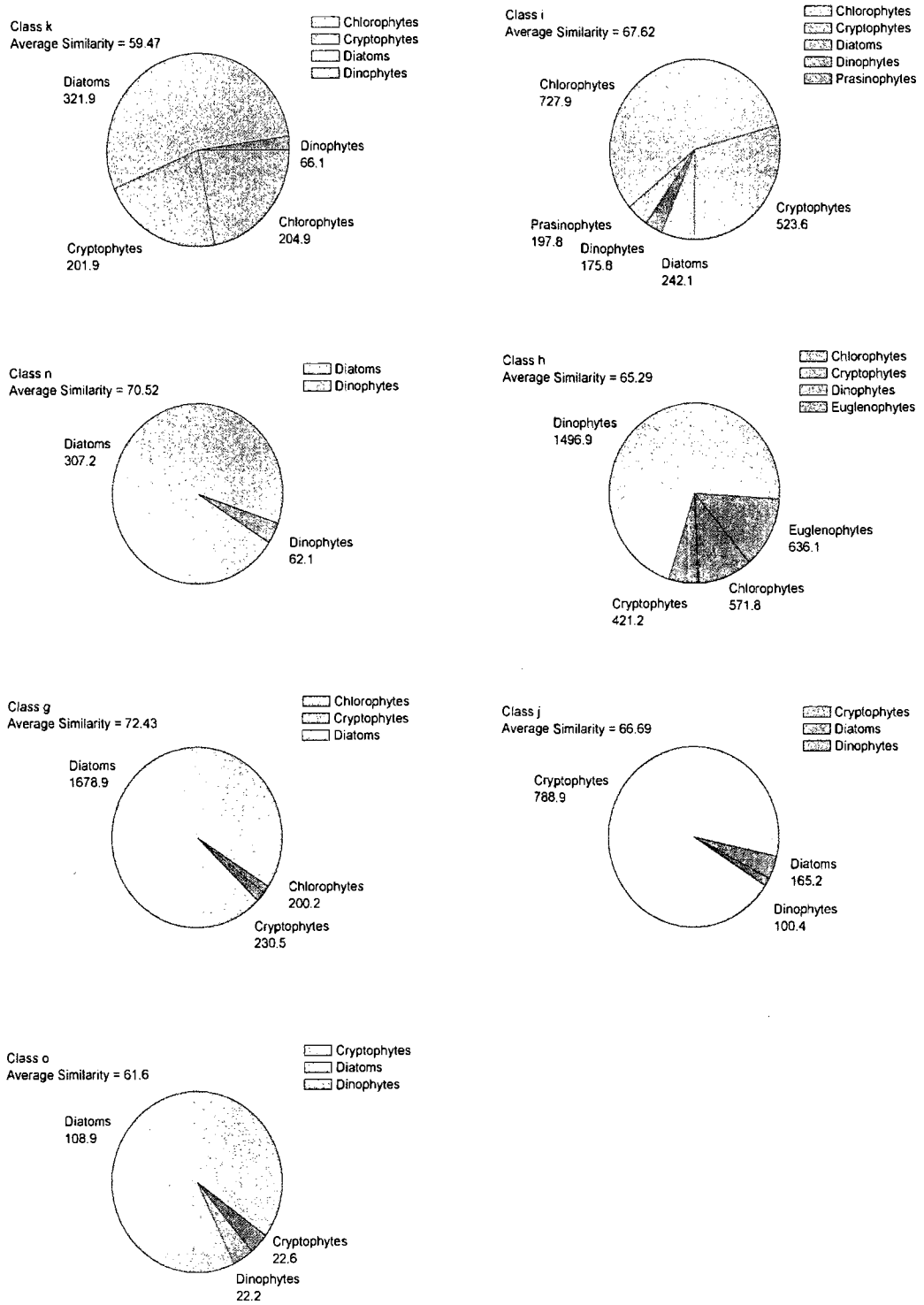


Figure 4. Pie graphs illustrating SIMPER analysis of the average abundance of taxa contributing to within site similarity. Data represented below class taxa is the average abundance within classes.

Seasonal shifts in phytoplankton populations were graphed by month and relative abundance (Fig. 5). Collections throughout the year often consisted of representatives of most classes, often with high numbers ($>10^8$ cells L^{-1}). Cryptophytes and chlorophytes were most abundant in summer months. Cryptophyte populations peaked in late summer and fall, with maximum population counts of $>2 \times 10^6$ cells L^{-1} . Chlorophytes were most abundant in middle to late summer, showing ranges similar to those of cryptophytes.

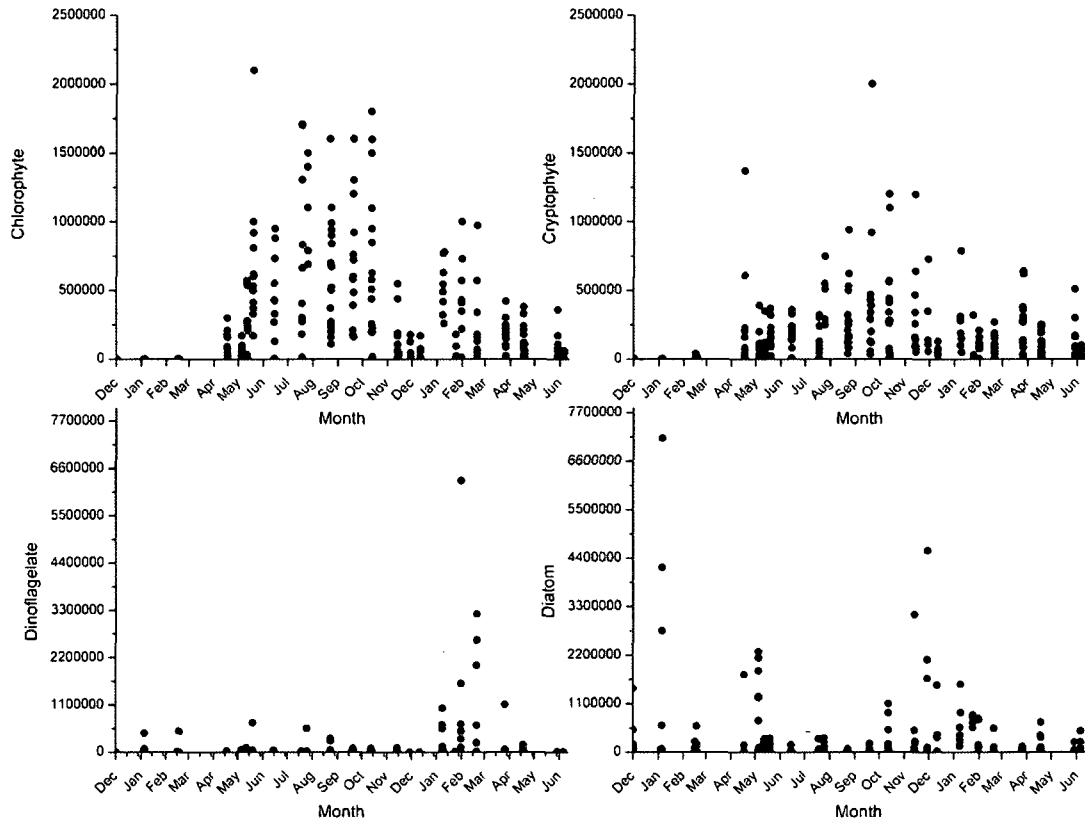


Figure 5. Relative abundance of diatom, chlorophytes, cryptophytes, and dinoflagellate collections. Charts show seasonal trends with diatom and dinoflagellate abundances higher in winter and spring, and chlorophytes and cryptophytes abundances higher in summer and fall months. Note difference in Y-axis between upper and lower panels.

Opposite trends existed within diatom and dinoflagellate populations. Diatoms peaked during late winter and early spring months, exhibiting highest maxima of class data (7×10^6 cells L^{-1}). Dinoflagellates exhibited similar population cycles with highest population peaks in early spring and maximum counts of $>6.5 \times 10^6$ cells L^{-1} .

Nutrient Analysis

PCA analysis used the classes as factors and the most relevant environmental variables as determined by draftsman plot analysis to determine the effects of environmental variables on phytoplankton populations. PC1 (Fig. 6) explains 53% of the variation between classes. The addition of PC2 shows a cumulative variation of 70.3%.

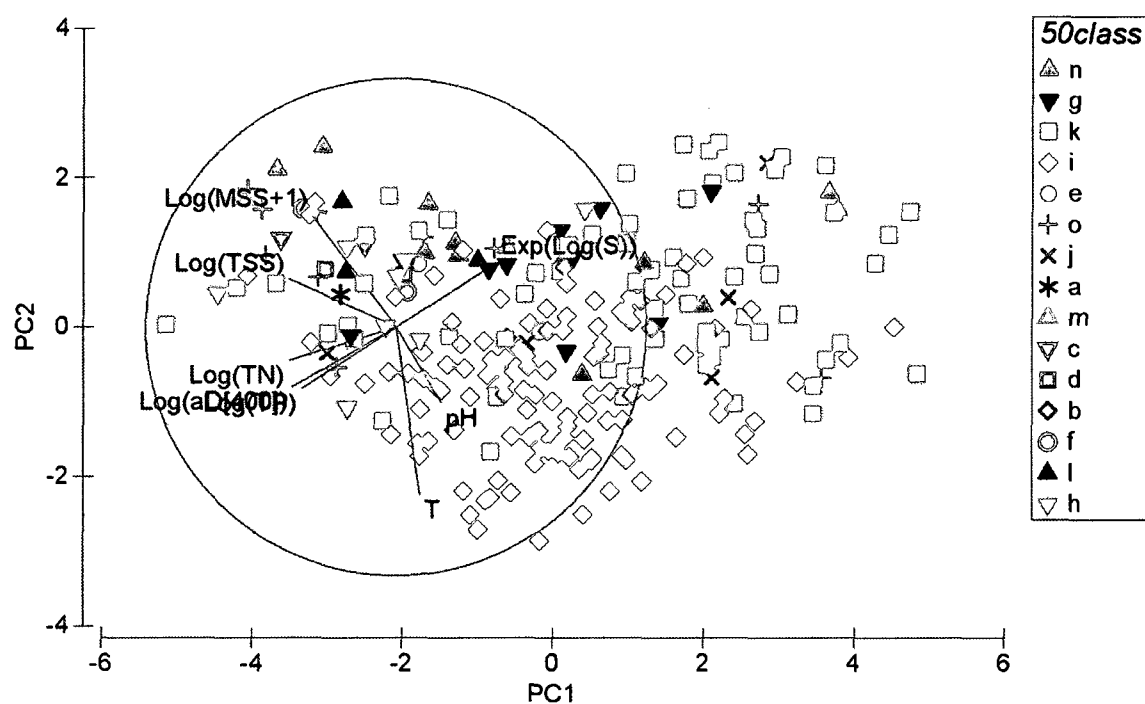


Figure 6. PCA analysis of S, T, pH, TN, TP, aD400, TSS, and MSS. Note the axes of the eigenvectors S, TN, and TP, and their orientation with the data classes i (red diamond) and k (blue square).

This represents a better than normal account of the factors most influencing the similarity between classes. Within PC1, the axis created by the eigenvectors of S (0.404), TN (-0.428), and TP (-0.376) fits well with the ordination of samples within the classes i and k. This axial plane and the respective values of the eigenvectors (Table 1) allow for a reduction of data from the original 8 variables to the 3 most applicable in explaining population counts in the classes, those being S, TN, and TP. These three factors were utilized in creation of graphs that illustrating relationships of water discharge and S, S and TN, and subsequent influence on nutrient distribution and phytoplankton populations.

Table 1

Eigenvalues and eigenvectors from PCA analysis in Figure 5

Eigenvalues

<u>PC</u>	<u>Eigenvalues</u>	<u>%Variation</u>	<u>Cum.%Variation</u>
1	4.24	53.0	53.0
2	1.38	17.3	70.3
3	0.886	11.1	81.4
4	0.63	7.9	89.3
5	0.548	6.8	96.1

Eigenvectors
(Coefficients in the linear combinations of variables making up PC's)

<u>Variable</u>	<u>PC1</u>	<u>PC2</u>	<u>PC3</u>	<u>PC4</u>	<u>PC5</u>
T	0.095	-0.677	-0.175	0.625	0.311
Exp(Log(S))	0.404	0.263	0.082	-0.015	0.546
pH	0.181	-0.305	0.886	0.022	-0.255
Log(TN)	-0.427	-0.135	0.126	-0.305	0.221
Log(TP)	-0.376	-0.246	0.137	-0.352	0.554
Log(TSS)	-0.428	0.193	0.251	0.340	0.100
Log(MSS+1)	-0.340	0.454	0.172	0.525	0.083
Log(aD[400])	-0.416	-0.241	-0.227	-0.010	-0.409

The station at Mid-Bay light in Mobile Bay was chosen as the primary site for the comparison of discharge, S, TN, and TP due to its centralized location and having the highest number of collections over the period of study (N=18). Trends exhibited by data at this station are similar to all collections sites in the study. Daily mean discharge (daily means of the total discharge ($\text{m}^3 \text{s}^{-1}$) of the Tombigbee and Alabama Rivers (combining to form the Mobile River), and Tensaw Rivers downloaded from the nearest upriver data collection site of the USGS National Water Information System website) were summed and compared to S, TN, and TP (Fig. 7), with concentrations of Chla used as a proxy for biomass. Results showed a high degree of response in S to discharge volumes and resultant swings in nutrient levels with high and low discharge levels causing low and high salinity readings. This response is consistent throughout the year, with high river discharge exhibiting a positive relationship with TN, TP, and Chla during the periods of high discharge volume, and corresponding lower nutrient and Chla levels with low discharge levels.

An inverse relationship between S and discharge is further illustrated in Figure 8, with fresh water input to Mobile Bay strongly influencing salinity readings at stations in the middle of Mobile Bay (Mid-Bay Lighthouse) and stations further from the influence of river discharge from the combined Mobile-Tensaw River system (east end of Dauphin Island, at the mouth of Mobile Bay). This inverse relationship exists at all stations within MB and throughout the study area, although the data are not shown. The response of S and the opposite response of TN, TP, and Chla, to the influence of fresh water and riverine and estuarine inputs of nutrients to the waters of the Mississippi Bight also is consistent throughout the study area.

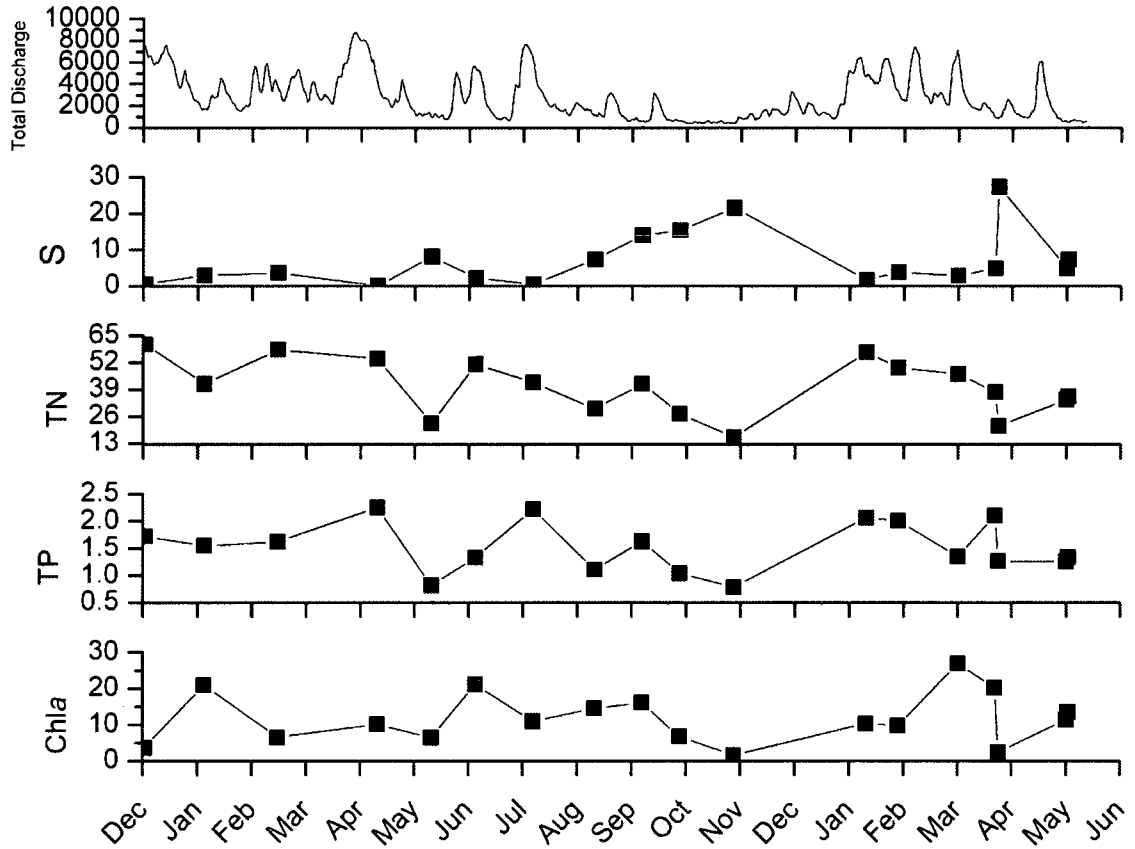


Figure 7. Stack graph with 5 panels showing the relative influence of total combined mean monthly discharge ($\text{m}^3 \text{s}^{-1}$) from the Mobile and Tensaw Rivers on S (psu), TN ($\mu \text{mol L}^{-1}$), TP ($\mu \text{mol L}^{-1}$), and Chla ($\mu \text{g L}^{-1}$) concentrations at the Mid-Bay Light station.

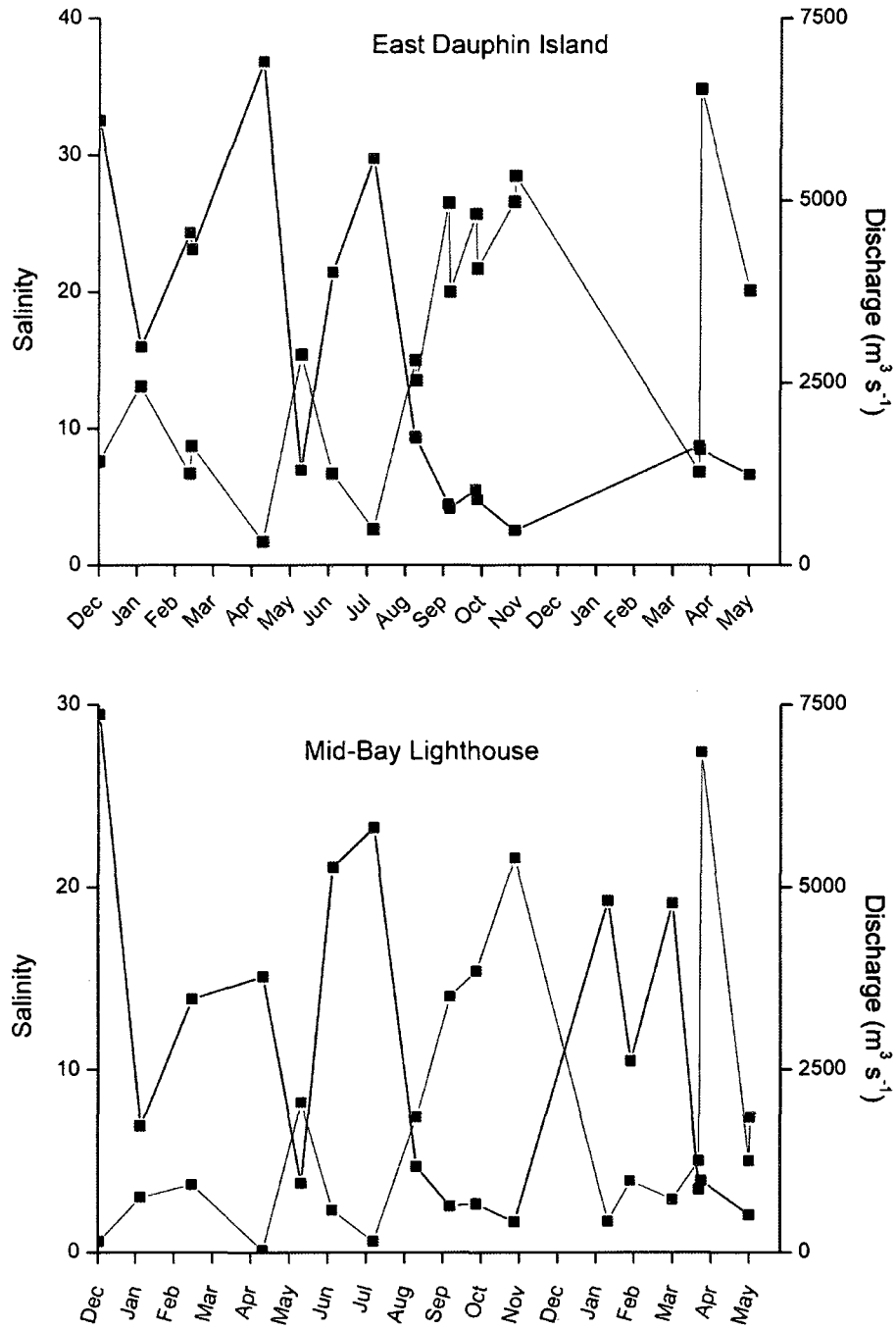


Figure 8. The relationship between S and discharge at Mid-Bay Lighthouse and the east end of Dauphin Island. Discharge values are averages of 14 days before collection date. Note the inverse relation between river discharge and salinity.

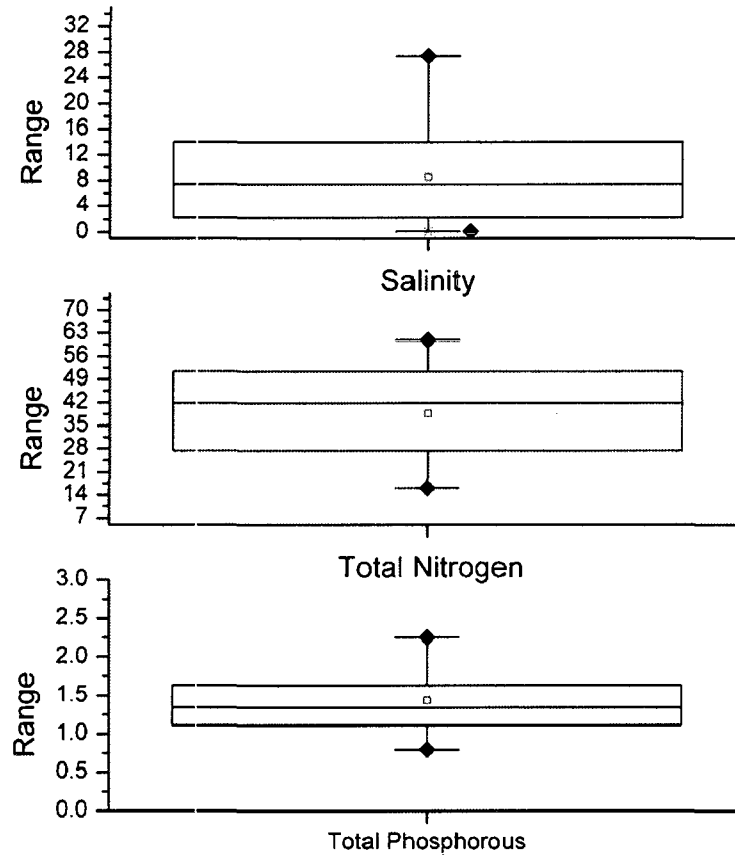


Figure 9. Box plots of S, TN, and TP, from all collections at Mid-Bay Lighthouse. The lower, middle, and upper lines of the boxes represent the first quartile, median, and third quartile, respectively. The bars extending from the boxes represent data range, black diamonds represent data maximum and minimum.

Box and whisker plots of ranges, first quartile, median, and third quartile readings, and outlier data from the Mid-Bay Lighthouse (Fig. 9) showed a range of near 0 to 31 psu and a median of 9 psu in S during the collection period, indicating a relatively constant low salinity level at this station. TN (Range=28-49 $\mu\text{ mol L}^{-1}$, median=38 $\mu\text{ mol L}^{-1}$) and TP (Range=1.2-1.7 $\mu\text{ mol L}^{-1}$, median=1.4 $\mu\text{ mol L}^{-1}$) showed higher relative concentration levels. This is consistent with the fact this station was strongly influenced

by river discharge levels causing relatively lower salinity levels and higher nutrient levels consistently throughout the collection period.

Conclusions

MB is dominated by freshwater inputs that can vary at hourly scales, creating a changing environment with abiotic and biotic variables subject to rapid change. In spite of these unstable conditions, this study has shown that patterns do exist within a framework of conditions that are seemingly difficult to predict. Phytoplankton populations, with individual collections consisting of millions of individuals per liter and numerous taxa, thrive within these nutrient rich waters. Inverse relationships between salinity and freshwater discharge and subsequent shifts in nutrient availability with nitrogen and phosphorous increasing as freshwater input increases, drive the seasonal population trends.

CHAPTER III
THE USE OF SEAWIFS DATA IN FORMING DECISION TREE MODELS TO
PREDICT BLOOMS OF PSEUDO-NITZSCHIA IN MOBILE BAY

Introduction

During the past three decades, continual development has been seen in the area of pattern recognition and classification of remotely sensed data (Pal & Mather, 2003). Research into algorithmic aspects of pattern recognition has proceeded alongside the development of both in situ and remote sensor instruments that are capable of producing high volumes of data, including images with increasingly finer spatial and spectral resolution (DeFries & Townshend, 1994; Pal & Mather, 2003). In recent years the use of decision tree modeling (DT) in remote sensing studies has increased. DT models are computationally fast, make no statistical assumptions, and are able to manage data represented on different measurement scales, factors which must be addressed when incorporating large, heterogenous data matrices such as those formulated using sensor imagery (Gahegan & West, 1998). In comparison to neural networks they may be trained quickly and with minimal data (Borak & Strahler, 1999), an important consideration when working with the small spatial scales of phytoplankton blooms in shoreline areas of the northern GoM.

Since its launch onboard the Orbview-II satellite in August 1997, the Sea-viewing Wide Field-of-view Sensor (SeaWiFS) has provided ocean color data products for use in global and local studies for the oceanographic community (Gordon & Franz, 2008; Gordon, Clark, Mueller, & Hovis, 1980; McClain, John, Karl, & Steve, 2009). Ocean color data are able to provide global or local information based on the spectrum of

radiation from the sun and sky that has penetrated the oceans surface and emerged from below after being scattered upward from subsurface depths. This recorded spectrum of upwelling water leaving radiance (L_w) is a result of the scattering and absorption of light measured at wavelengths in the visible and near infrared regions and is influenced by the concentration and optical properties of the organic and inorganic constituents of seawater (Gordon et al., 1980; Green, Gould, & Ko, 2008). Another commonly used parameter in the field of ocean color is the remote sensing reflectance, R_{rs} , which is defined as the ratio between the upwelling radiance, L_w , just above the water surface to the downwelling irradiance, E_d , at the same level. R_{rs} is a function of wavelength, λ , as well as the viewing angle (IOCCG, 2000; Johnson, 1978). In Case I waters variations in $a(\lambda)$ and $bb(\lambda)$ are due to phytoplankton only (McClain, Feldman, & Hooker, 2004; Morel & Gentili, 1991). Consequently, these measurements are used to interpret the gradations of ocean color from blue to green as proxies for concentrations of phytoplankton within the area of study (Gordon et al., 1988; McClain et al., 2009). These reflectance measurement products are the foundation of remote sensing data, all ocean color algorithm products and data studies are reliant upon their usage. The use of the SeaWiFS sensor for primary production (Wawrick & Paul, 2004) and phytoplankton studies (Stumpf et al., 2009; Tomlinson et al., 2009) have shown the utility of R_{rs} data in carrying out synoptic and rapid coverage of regional waters, improving the recognition and response time to potential HA events.

Anderson et al. (2008) showed that increase in coastal water nutrient loads correlated directly with increased microalgal populations. As human populations increase in the Mobile Bay and Mississippi Sound regions, anthropogenic nutrient loading will rise correspondingly (Baya et al., 1998; USEPA, 1999), demonstrating a need for

economical and efficient means of HAB detection and prediction in the northern GOM. The focus of this study was to develop an integrative DT prediction model that can utilize specific products of readily available SeaWiFS reflectance data products to predict the occurrence of phytoplankton populations in the region in and near MB.

Methods

Phytoplankton Population Description

Surveys carried out in Alabama waters by Pennock et al. in 2001 and 2002 and routine surveys done by Dauphin Island Sea Lab (DISL) and the Alabama Department of Public Health (ADPH) regularly identify species of microalgae, mostly dinoflagellates and diatoms, with the potential to create HAB events (unpublished data, ADPH). To date, 5 known toxin-producing HAB species have been detected at significant levels ($>10^5$ cells L^{-1}) in coastal waters of the northern GOM. These include the diatoms *Pseudo-nitzschia* spp. and the dinoflagellates *Karenia brevis*, *Gymnodinium sanguineum*, *Dinophysis caudata*, and *Prorocentrum minimum*. *Karlodinium veneficum*, a producer of karlotoxins, and *Heterocapsa triquetra*, a dinoflagellate found in high cell concentrations leading to hypoxic conditions, have caused fish kills in MB (Bill Smith, ADPH). Other potential HAB species, such as the dinoflagellates *Karenia mikimotoi*, associated with massive fish kills in Japan and Korea, and two members of the genus *Gonyaulax*, *G. digitale* and *G. polygramma*, associated with non-toxic red tides in Florida (Landsberg, 2002) have been found at low levels (<2000 cells L^{-1}). The members of the genus *Pseudo-nitzschia* were chosen as the taxa used during the formation of this DT due to the potential of this genus for production of domoic acid (Bates & Trainer, 2006; Maier Brown et al., 2006) and the relatively high numbers, seasonal aspects of occurrence, and

frequency with which they have been collected in this region (Dortch et al., 1997; Liefer et al., 2009).

Phytoplankton Collections

Surface water samples were collected at 4-6 week intervals from December, 2004, through June, 2006, at 17 sites (N= 120) that encompass the major hydrographic regimes in southern Mobile Bay and its adjacent waters in the Mississippi Sound (Fig. 10). The stations were situated near Dauphin Island and Cedar Point, within Bon Secour Bay, and near Little Lagoon and the Ft. Morgan Peninsula, (an area of high cell concentrations, see Liefer et al., 2009).

One liter of surface water was preserved immediately upon collection with Lugol's solution. Identification and enumeration of phytoplankton species were determined by the Alabama Department of Public Health (ADPH) using inverted light microscope. Diatoms, dinoflagellates, chlorophytes, prasinophytes, euglenophytes, cryptophytes, dictyophytes, chrysophytes, and raphidophytes were enumerated in a settling Nunc chamber, only diatoms and dinoflagellates identified to species.

SeaWiFS Data

SeaWiFS data was obtained from the Naval Research Laboratory Offices, Code 7330, Ocean Sciences Branch, at Stennis Space Center, Mississippi (NRL). The 1 km resolution imagery was processed with the Naval Research Laboratory's Automated Processing System (APS). APS Version 3.5 utilized atmospheric correction algorithms proscribed by NASA's fifth SeaWiFS reprocessing, and includes a near-infrared (NIR) correction for coastal waters (Gordon, 1995; Stumpf et al., 2003). The NIR atmospheric correction method used by APS improves estimates of bio-optical parameters in

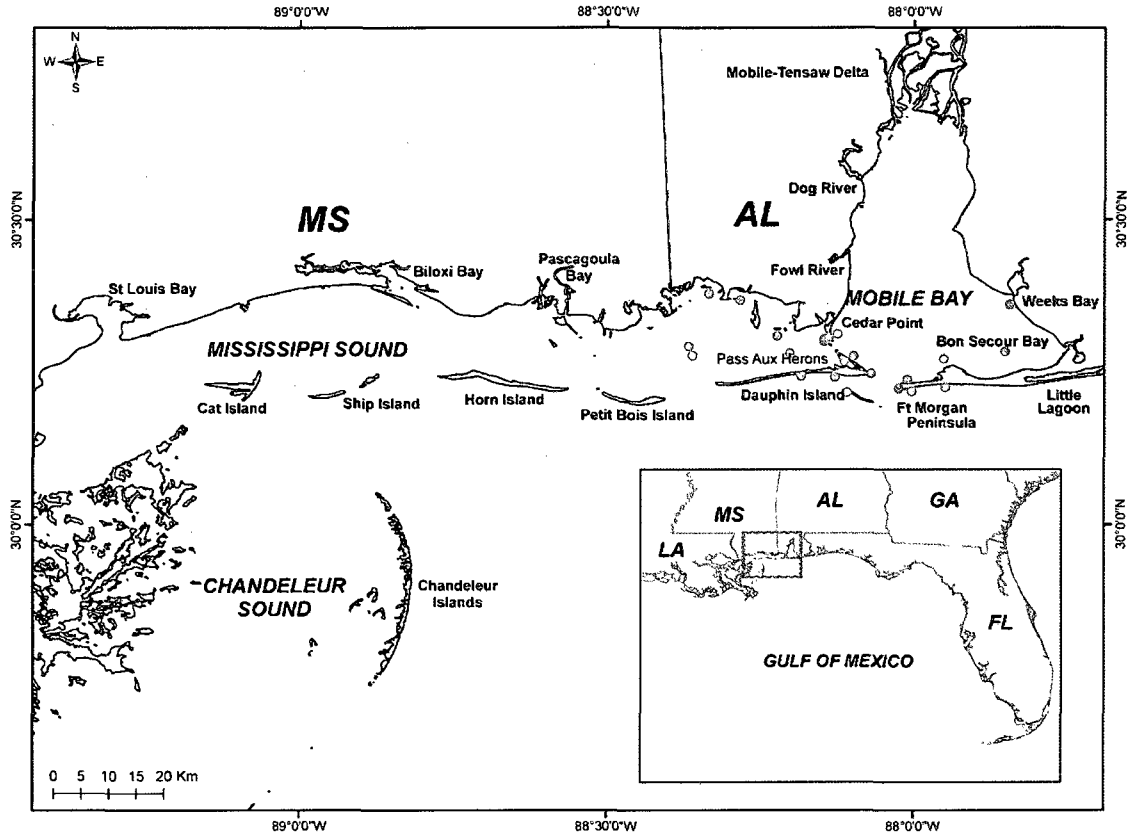


Figure 10. Map of collection sites in Mobile Bay, AL, and the eastern Mississippi Sound. *Pseudo-nitzschia* spp. population data from sites marked in solid gray were used in DT formation and testing. Sites from this area of Mobile Bay and surrounding waters were used due to maximum values of population data and common presence of *Pseudo-nitzschia* spp. within collections.

coastal regions by applying an iterative technique in which water-leaving radiance at 765 nm and 865 nm is estimated from water-leaving radiance at 670 nm. An absorbing aerosol correction was also applied to improve underestimates of satellite-derived water reflectance (Ransibrahmanakul & Stumpf, 2006). Weekly composites were used due to high percentage of cloud coverage or other aerosol interference in the region. Mobile, Alabama, is listed by the Weather Service as the rainiest city in the United States, with an

annual average rainfall of 67 inches and 59 rain days (National Weather Service, 2005). Field collections were undertaken 32 days during the 18 month collection period, with same-day SeaWiFS imagery available 12 of those days.

Decision Tree Development and Evaluation

DT is a type of modeling technique that provides qualitative discrete outputs of a database under certain conditions represented by those data. These outputs are represented by parameters used in challenging those data products with a simple statement (Solomatine & Dulal, 2003). It splits products, or outputs, of those statements into sub-domains for which the output of each is determined by the nature of the statement. Each statement is termed a node, each product of the statement a leaf. The DT classifier function of ENVI v4.3 was used to construct the model (Fig. 11). This function performs multistage classifications by using a series of binary decisions (the statement within the nodes) to place pixels into classes (sub-domains represented by leaves). The challenge of the statement within each node divides the pixels in an image into two leaves. The products of the leaves are represented by a numerical output of total pixels affected by the statement and the percentage of pixels surviving the challenge of the statement of each node. The final output is visually represented by a raster image mapping the placement of surviving pixels. In this model, the parameters of the challenge are derived from statistical analysis of the R_{rs} values from the SeaWiFS sensor and their relationship with population counts of the diatom genus *Pseudo-nitzschia*.

TableCurve 2-D v5 was used to determine variables used in formation of the nodes of the model. Threshold levels of wavelengths (412, 443, 488, 531, 551, and 670 nm) and all quotients derived from ratios of wavelength products were tested using

Gaussian algorithms with least-squares minimization applied to outputs. Only those quotients yielding an $R^2 \leq 4$ were used in formation of binary decisions decision tree nodes. Ratio quotients of 670/555, 555/443, and 555/490 were used in model formation.

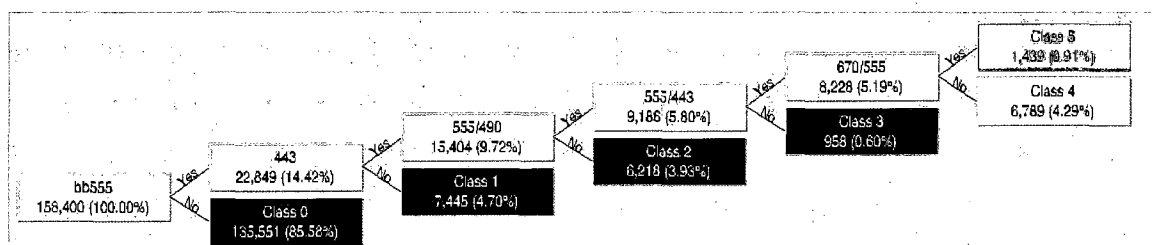


Figure 11. Visualization of Decision Tree classifier from ENVI v4.3. Notice titles of nodes indicating factors used in formation of the statement for the node, while percentages within each leaf represent number of pixels affected by the statement. This output is a result of the test performed on figure 3.D., showing 0.91% of pixels (1,409 of 158,400) having the unique set of environmental properties enabling *Pseudo-nitzschia* spp. to be present in high population numbers.

Subsets of *Pseudo-nitzschia* spp. data were used in formulation and validation of the decision tree. Collections from 05/06/2005 and 05/11/2005 (N=21) were used as training sites for development of the decision tree due to high cell counts (range 6,800- 1.5×10^6 cells L^{-1}).

Results

Thresholds of *Pseudo-nitzschia* spp. counts when related to R_{rs} data were noted early in the analysis of collection data (Fig. 12). Wavelengths of 670, 555, and 443 nm exhibited Gaussian relationships in analysis with population data. These relationships

improved as quotients of R_{rs} wavelength products were computed and those quotients applied to analysis. No similar relationships were noted in standard SeaWiFS algorithm products such as Chla, attenuation, or TSS, thus these products were not used in formation of the DT.

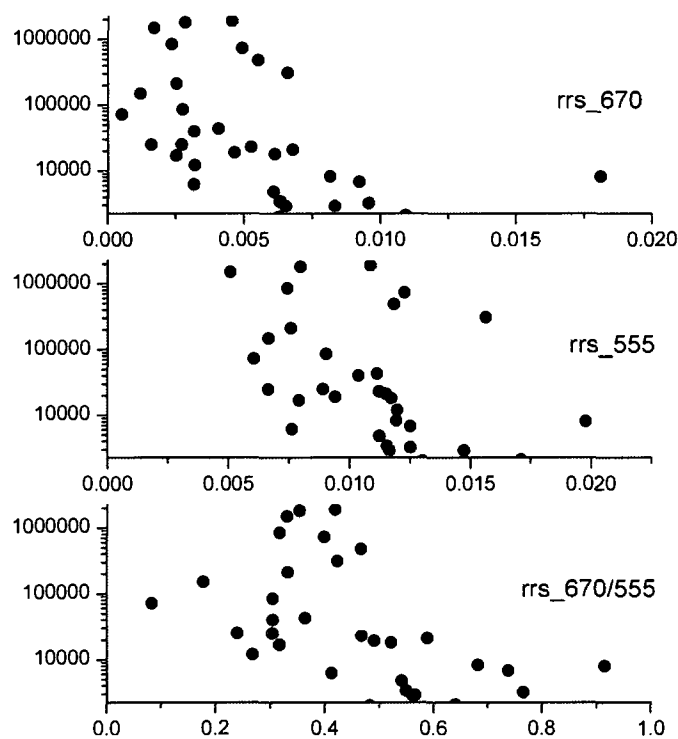


Figure 12. SeaWiFS R_{rs} products at 555 and 670nm, and quotient of these wavelengths at 670/555, with *Pseudo-nitzschia* spp. (cells L^{-1}) represented on the y-axis, natural log scale applied to data for allowing observation of cell numbers $>10^4$ cells L^{-1} . Note the spread of data points $<10^4$ at all wavelengths, and narrowing of data range when a 670/555 nm ratio is applied to R_{rs} data.

DT results were based on a per-pixel comparison of image data. Errors of omission were computed by applying regions of interest to pre- and post-testing images. Total number of pixels corresponding to field data collections of *Pseudo-nitzschia* spp.

populations are shown on final classifications of output imagery (Fig. 13), and percentage of pixels misclassified by the model were counted as errors of model output. The model exhibited an average error of omission rate of 21%, and average accuracy rate of 79% in testing of 10 collection periods. The results indicated a trend toward offshore motion of waters corresponding to high ratio quotient products (Fig. 13B & 13D).

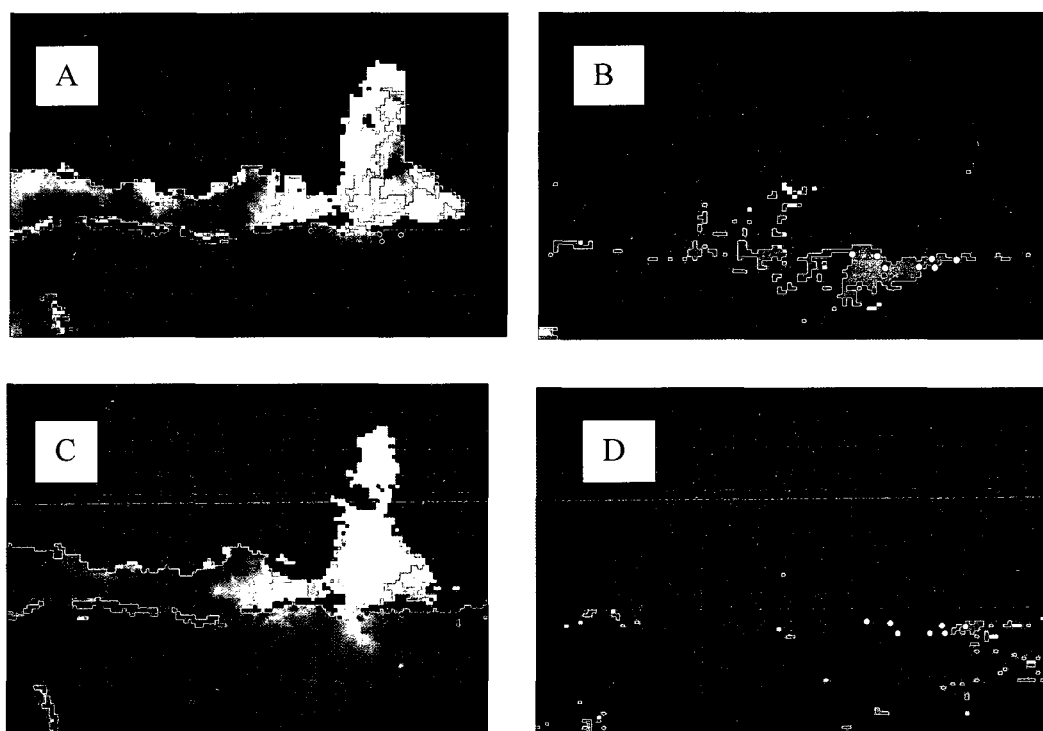


Figure 13.A. SeaWiFS image from May 6, 2006, R_{rs} at 670 nm, 1 km resolution. Red dots indicate locations of in situ collections.

B. Results from decision tree analysis, using *Pseudo-nitzschia* spp. counts from May 6, 2006. White dots indicate location of in situ data collections, spatial coverage is identical to Figure 3A.

C. SeaWiFS image from April 4, 2005, R_{rs} at 670 nm, 1 km resolution. Red dots indicate locations of in situ collections.

D. Results from decision tree analysis, using *Pseudo-nitzschia* spp. counts from April 4, 2005. White dots indicate location of in situ data collections, spatial coverage is identical to Figure 3C.

Discussion

This model represents an elegant and relatively simple method of tracking waters and the inherent environmental conditions leading to the formation of harmful algal blooms. It is computationally simple, uses satellite data input products that are provided without cost and obtained, processed, and extracted to usable form for model input with relative ease by users of the NASA Ocean Color website. Also, it is capable of being automated by computer programming, and may be adjusted for accuracy with changing water conditions if a different region of the collection territory is to be monitored.

CHAPTER IV
THE USE OF IN SITU REMOTE REFLECTANCE DATA TO FORM REGIONAL
ALGORITHMS FOR SALINITY PREDICTION

Introduction

Estimating phytoplankton biomass and distribution through quantifying and mapping nutrient concentrations in near shore environments has been a major application of remote sensing in coastal waters (Harding, Itsweire, & Esaias, 1994; Stumpf et al., 2009). The concentration of Chl_a is often used as a proxy of the phytoplankton biomass, and is essential in mapping the biological activity at the ocean surface, including monitoring of algal blooms and estimation of primary production (Antoine, Andre, & Morel, 1996; O'Reilly et al., 1998; Stumpf et al., 2009). Remote sensing studies involving phytoplankton are based on the study of ocean color, which is determined by absorption and scattering of visible light by the pure water component of the ocean as well as by the inorganic and organic, particulate and dissolved, materials present in the water (Behrenfeld & Falkowski, 1997; McClain et al., 2009; Siegel et al., 2005). The influence of salinity gradients in the distribution of these constituents has been emphasized in numerous studies (Quinlan & Philips 2007; Marshall et al., 2006; Muylaert et al., 2009), with the contribution of estuarine DOC and CDOM of riverine origin being of major importance to the formation of salinity gradients (Del Castillo & Miller, 2008; D'Sa, Miller, & Del Castillo, 2006). Formation of regionally specific algorithms for the purpose of predicting CDOM and salinity values are important for inputs to HAB prediction models based solely on remote sensing values, and none presently exist for this region. This study involves the use of remote sensing reflectance (R_{rs}) as measured in situ

during two cruises within the Mississippi Sound to compute regional specific algorithms for use in satellite-derived salinity values.

An Explanation of Remote Sensing Reflectance

When dealing with Case I, or open ocean, waters, pure water and phytoplankton are the dominant components influencing the remote sensing signal (Mobley, 1999; Morel & Prieur, 1977). In these waters, the optical contribution from components such as DOC and CDOM are minimal. In contrast, Case II waters are defined to contain numerous components derived from riverine and terrigenous inputs that vary independently of chlorophyll, and in such amounts that they significantly influence the optical properties in the water (Del Vecchio & Blough, 2002; IOCCG, 2000). Case II waters are generally found in inland and coastal water bodies, carrying CDOM and DOC from terrestrial sources by river runoff (Johannessen, Miller, & Cullen, 1999).

The measurement of these water properties is reliant upon R_{rs} , which is defined as the ratio between the upwelling radiance (L_w) just above the water surface to the downwelling irradiance (E_d) at the same level (Mobley, 1994). R_{rs} is a function of wavelength (λ) as well as the viewing angle. Studies have shown that R_{rs} can be expressed in terms of the absorption coefficient ($a(\lambda)$) and the backscattering coefficient ($bb(\lambda)$) in the water (IOCCG, 2000; Gordon & Franz, 2008). In Case I waters variations in $a(\lambda)$ and $bb(\lambda)$ are due to effects of phytoplankton only (Morel & Prieur, 1977; Carder et al., 1999). Consequently, simple empirical relationships can be established between $Chl a$ and variations in R_{rs} , when a large number of concurrent in situ measurements of these two parameters are utilized (Morel & Gordon, 1980; O'Reilly et al., 1998). However, in Case II waters, CDOM, organic and inorganic constituents, and

phytoplankton contribute to $a(\lambda)$ and $bb(\lambda)$ and do not conform to their inputs (IOCCG, 2000). However, the contribution to $a(\lambda)$ and $bb(\lambda)$ from each of these constituents are additive, and can for each be expressed as the product between the concentration of the constituent and its concentration-specific absorption and backscattering coefficients, respectively. These coefficients are collectively termed inherent optical properties (IOP) (Hoge et al., 2001; Kuchinke et al., 2009; Mobley, 1994). The IOP are functions of the wavelength, and can vary substantially between different water bodies containing various types of constituents (IOCCG, 2000; Morel & Gentili, 1996). Even though expressions relating the IOP and in-water constituent concentrations to R_{rs} theoretically can be universally applicable for Case II waters, the coefficients of IOP, and products relying upon this input, must be determined for each water body in question.

Studies have shown the importance of salinity in understanding the spatial and temporal relationships among phytoplankton populations (Quinlan & Phlips, 2007; Muylaert et al., 2009; Wawrick & Paul, 2004). Ocean color remote sensing has been shown to provide reasonable estimates for salinity in the nearby Mississippi River plume (Del Castillo & Miller, 2008; D'sa, Miller, & Del Castillo, 2006) based solely on R_{rs} ratios and empirical algorithms. The purpose of this study is to provide a salinity algorithm based on R_{rs} data from the SeaWiFS ocean color sensor specific to the waters of the MS.

Methods

Study Site Description

The MS (30.2 N, 88.3W) is a shallow coastal lagoon with a mean depth of 3 m, approximately 130 km long and 11-24 km wide, bordered on the south by a series of

barrier islands and on the north by the mainland shoreline of Mississippi (Wilber et al., 2007). Waters from the MS are generally well-mixed with minimal difference between surface and bottom temperature and salinity (Dinnel & Schroeder, 1989). The MS is influenced by groundwater discharge and inputs from the Pascagoula, Escatabwa, and Biloxi River systems and MB discharge (Loyacano & Smith, 1979). The MB estuary (30.5 N, 88.0 W) is a drowned river system, approximately 50 km long with a width of up to 31 km (Schroeder, 1977). It is a shallow (average depth 3m), highly stratified estuary with a surface area of approximately 1,070 km², a relatively small volume of 3.2 X 10⁹ m³ and a short residence time of days to weeks (NOAA/EPA, 1989). MB is dominated by nutrient laden freshwater inputs of riverine and groundwater discharge origins (Loyacano & Smith, 1979). At the north end of MB, the Mobile River is formed by the confluence of the Alabama and Tombigbee Rivers, combining to form the fourth largest watershed in the coterminous United States (Bricker et al., 2007). This system dominates water flow into the bay, contributing 95% of freshwater input (Schroeder et al., 1979). The addition of freshwater from the Dog and Fowl Rivers on the west shore and Fish and Magnolia Rivers flowing into Weeks Bay along the east shore create an average daily freshwater input of 1.56 x 10⁸ m³ d⁻¹ (Engle et al., 2007), and short freshwater fill time of approximately 20 days (Cowan et al., 1996). Average monthly discharge rate into the northern GoM is 1,800 m³ s⁻¹ (for the period from 1929 to 1983, see Schroeder & Wiseman, 1986).

Fieldwork

Water samples and above water optical measurements were collected at 22 stations (Fig. 14) during two cruises to the Mississippi Sound on October 25 and 26,

2007. Skies were overcast the morning of the first day with afternoon clearing, but clear the second day, permitting measurements during simultaneous satellite overpasses.



Figure 14. Locations of stations used in collection of water samples, in situ spectroradiometer readings, and SeaWiFS data extractions.

Spectroradiometer Readings and Optical Measurements

Above-water remote sensing reflectance at 1-nm intervals between 400 and 825 nm were recorded using an Ocean Optics Spectroradiometer, following the measurement protocol of Mueller and Austin (1995). Above-water remote sensing reflectance, $R_{rs}(\lambda)$, was derived according to Mueller and Austin (1995). Radiance spectra were recorded from surface waters ($L_{\lambda_{sea}}$), followed by measurements of sky radiance ($L_{\lambda_{sky}}$) and atmospheric radiance using a 98% reference Spectralon placard (Labsphere). All measurements were taken five times. R_{rs} at wavelength

$(R_{rs}(\lambda))$ was calculated as

$$R_{rs}(\lambda) = ((L_{\lambda,sea} - \rho(\theta)L_{\lambda,sky}) / (\pi L_{pl} / \rho_{pl})) - L_{residual-750} \quad (1)$$

where ρ (0.025) is the Fresnel reflectance at the viewing angle θ (30°), ρ_{pl} is the reflectance of the Spectralon, and $L_{residual-750}$ is the R_{rs} at 750 nm subtracted to remove any residual reflected radiance from the sky.

Water Sampling and Analysis

Water samples for CDOM analyses were collected simultaneously with the optical measurements. CDOM samples were filtered using 0.22 μm membrane filters mounted on polycarbonate apparatus. Filters were pre-rinsed with methanol and nanopure water. The filtration system was flushed with approximately 20 ml of sample water before measurement of CDOM samples.

Absorption Spectroscopy

Absorption spectra of filtered samples were obtained between 250 and 700 nm at 1-nm intervals using a Perkin Elmer Lambda-18 double-beam spectrophotometer equipped with matching 10-cm quartz cells. Nanopure water was used in the reference cell. The absorption coefficients, $a(\lambda)$, were calculated using $a(\lambda) = 2.303A(\lambda)/l$, where A is the absorbance ($\log_{10}(I_0/I)$) and l is the path length in meters. Absorption at 412 nm was used as an index of CDOM concentration and will be referred to as a_{g412} .

Results

Field Samples

Table 2 shows station information and salinity and a_{g412} values for all field samples used in the study. Note the inverse relationship between salinity and a_{g412} , indicating a conservative relationship. The CDOM absorption spectra obtained from the

water samples (Fig. 15) shows a wide range of CDOM absorption properties indicating the data set is representative of the water types found in the MS, consistent with previous work in coastal areas of the Gulf of Mexico (Del Castillo, 2005; Del Castillo & Miller, 2007). Best fit functions were derived using TableCurve 2D v5 (SYSTAT Software). Best fit exponential and linear equations are shown, with the exponential function returning marginally improved results (Fig. 16) of $R^2 = .93$ as opposed to $R^2 = .9$ for the linear equation.

Table 2

Station information, salinity and CDOM values. Note the inverse relationship between salinity and a_{g412}

Station ID	Date	Time ¹	Latitude	Longitude	salinity	ag 412 nm
s11	10/25/2007	10:00	30.326	88.756	18	3.712
s10	10/25/2007	10:25	30.308	88.602	28	0.928
s9	10/25/2007	11:00	30.286	88.157	27	1.193
s5	10/25/2007	11:20	30.243	88.340	31	0.675
s6	10/25/2007	11:50	30.270	88.250	32	0.398
s8	10/25/2007	12:35	30.338	88.343	29	0.861
s12	10/25/2007	13:40	30.336	88.658	25	1.796
O1	10/26/2007	10:25	30.200	88.775	33	0.366
O2	10/26/2007	10:40	30.156	88.775	35	0.235
O3	10/26/2007	10:55	30.055	88.770	35	0.251
O4	10/26/2007	11:06	30.103	88.726	35	0.267
O5	10/26/2007	11:25	30.100	88.667	35	0.214
O6	10/26/2007	11:40	30.150	88.672	29	0.877
S1	10/26/2007	12:10	30.255	88.774	30	0.686
s13	10/26/2007	12:40	30.300	88.767	26	1.271
s14	10/26/2007	13:00	30.285	88.834	25	1.460

¹Local time

Optical Measurements

Weather conditions were favorable for the collection of water measurements of radiance and solar irradiance. Low winds and calm waters created surface water conditions without whitecaps that reflect light and negatively affect spectroradiometer measurements. Day one was completely overcast in the AM with clear afternoon skies, day two had clear skies. Figure 12 illustrates all R_{rs} spectra generated from in situ spectroradiometer field measurements. The data show the variability in optical conditions found in the study area, with R_{rs} values at 555 nm ranging from .01 to .08 l/sr with changing in situ conditions. MODIS and SeaWiFS data were comparable across all stations (Fig. 17). Most variability was caused by spectroradiometer measurements of water reflectance. The variability in sky and placard measurements was negligible for most stations (data not shown).

Remote sensing measurements of R_{rs} done with SeaWiFS and MODIS-Aqua compared well with field measurements (Fig. 18). Comparison between spectroradiometer and MODIS measurement values yielded $R^2 = .87$, with SeaWiFS showing only slight improvement ($R^2 = .89$). These results are exceptional considering that only stations O6, S1, S13, and S14 were within two hours of a satellite overpass. Furthermore, these spectroradiometer measurements represent points within a 1 km² pixel in a highly variable coastal environment, as opposed to the multi-spectral satellite sensor remote sensing measurement consisting of the mean of a 1 km² pixel.

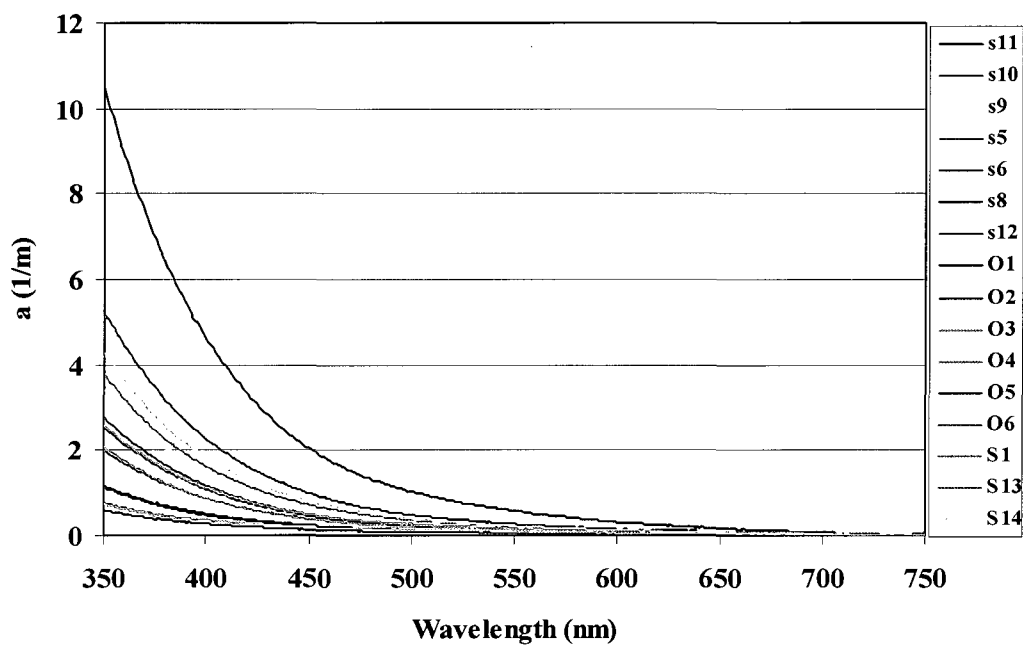


Figure 15. Absorption spectra of CDOM obtained from samples collected in the MS.

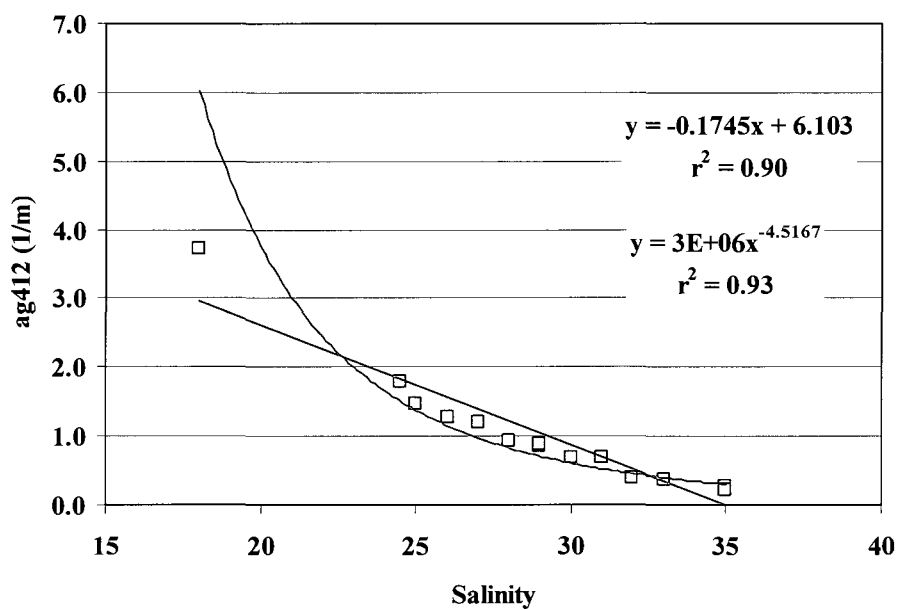


Figure 16. $a_g 412$ vs. salinity from samples collected in the Mississippi sound. stations (data not shown).

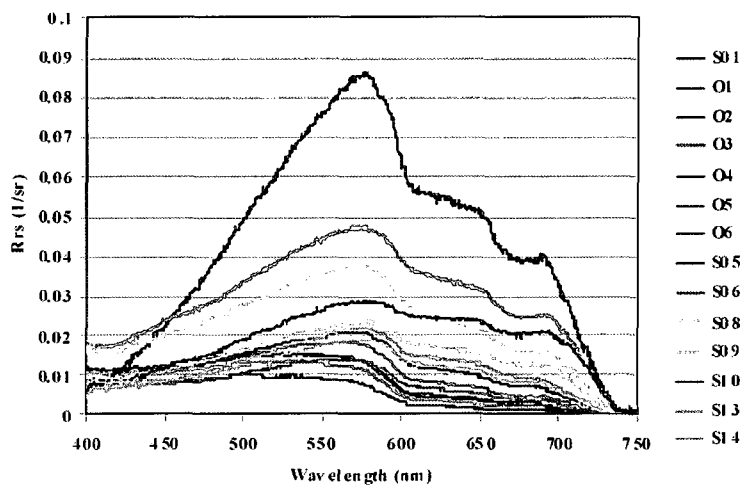


Figure 17. R_{rs} data collected from in situ stations in the MS.

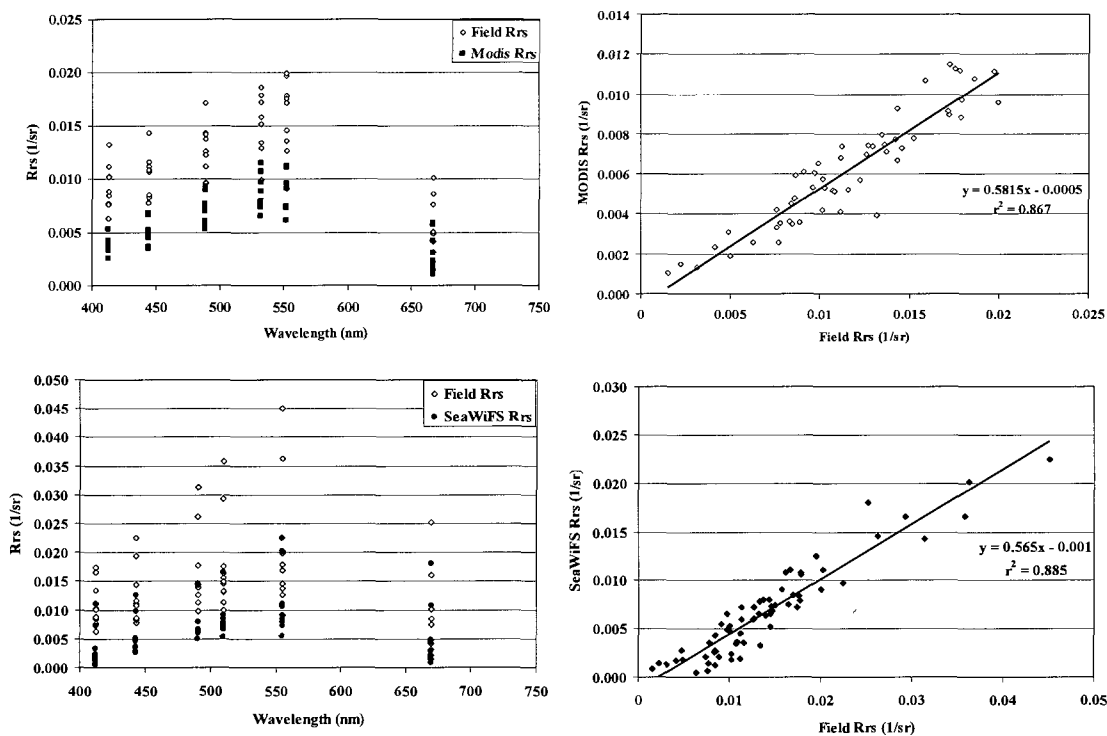


Figure 18. Comparison between field and remote sensing measurements of R_{rs} . Field and remote sensing images were collected on October 25 and 26, 2007. Linear equations developed using TableCurve v5. Note $R^2 = .87$ using MODIS data, and $R^2 = .89$ using SeaWiFS data. Spectroradiometer field data and corresponding R_{rs} sensor data show ranges of <0.025 1/sr.

Algorithm Development

Field spectroradiometer data and laboratory measurements of $a_g(412)$ and salinity were used to develop empirical algorithms for the region, with best fit functions determined using TableCurve 2-D v5. The algorithms are based on the ratio of 510 nm to 555 nm, valid only for SeaWiFS data. The ratio of 510 nm/555 nm was chosen because it had previously been successfully used in coastal waters of the Gulf of Mexico (Del Castillo & Miller, 2007), and SeaWiFS data are available since 1997, enabling the option of determining salinity for archived data. The SeaWiFS CDOM algorithm is a power function of the form

$$a_g(412) = 0.2953(R_{rs\ 510}/R_{rs\ 555})^{-4.1464}$$

and the salinity algorithm is a linear function of the form

$$salinity = 23.975(R_{rs\ 510}/R_{rs\ 555}) + 9.967$$

SeaWiFS images (Fig. 19) of the Mississippi Sound from October 26, 2007, are provided. These images were processed using the Ocean Biology Processing Group at NASA Goddard Space Flight Center SeaDAS v5.4 software, and represent processing using the $a_g(412)$ and salinity algorithms developed within this work.

Conclusions

Empirical algorithms were generated to estimate values of salinity and $a_g(412)$ in the Mississippi Sound. The algorithms are based on the wavelength ratio of $R_{rs\ 510}$ to $R_{rs\ 555}$. Comparisons between field and remote sensing measurements of R_{rs} are acceptable for both MODIS and SeaWiFS, with R^2 values of .87 and .89, respectively. A small spectral bias exists between spectroradiometer and satellite remote sensing measurements, and between SeaWiFS and MODIS sensor products. Therefore, a multi-

sensor approach can be used in the area to increase remote sensing coverage for salinity and CDOM, compensating for lack of coverage by either sensor caused by split-scene or other anomalies.

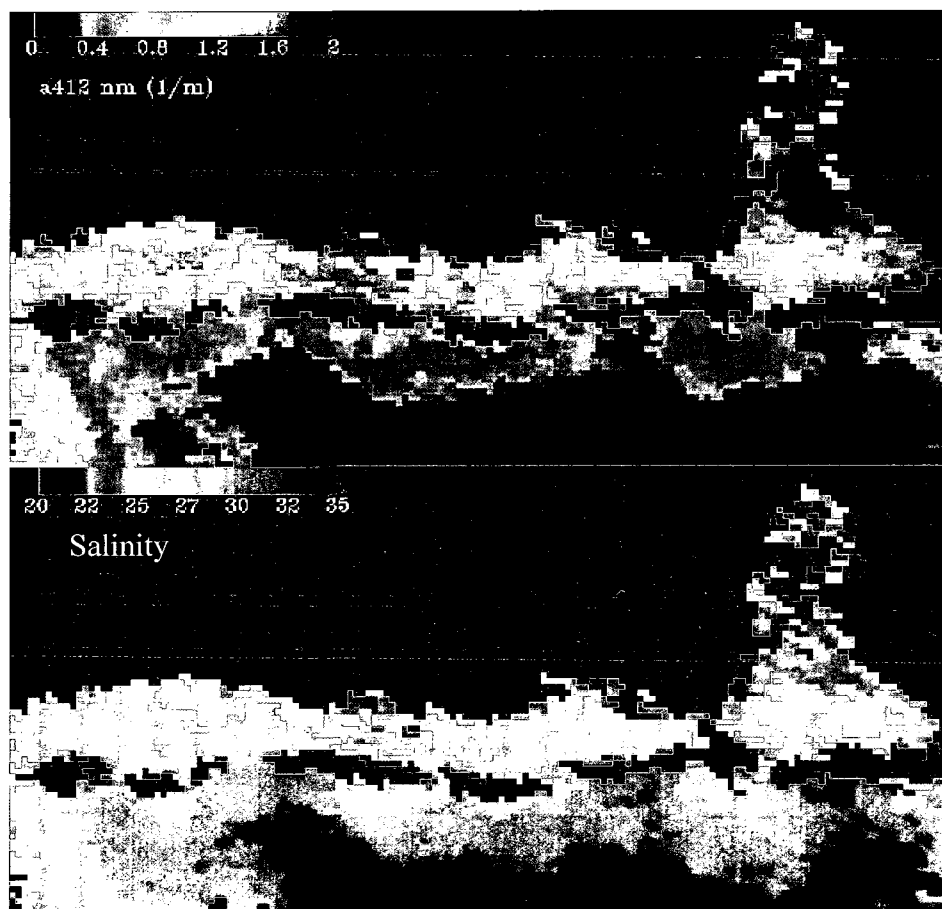


Figure 19. Remote sensing retrievals of a_{g412} and salinity based on empirical algorithms developed in this work. Images are based on SeaWiFS data collected on second collection day, and processed using SeaDAS v5.4.

CHAPTER V

SUMMARY

Spatial and temporal patterns in phytoplankton populations are a result of response to ecological conditions within their environment. In order to understand how blooms of phytoplankton, particularly potential HA species, form in the diverse and rapidly changing conditions present within the northern GoM we must work toward a better understanding of the conditions that create, maintain, and disperse these populations. The use of remote sensing data from sensors such as SeaWiFS have been shown to be of utility in other regions of the GoM, and this study shows their potential in this optically complex region.

Chapter II analyzed the species composition of phytoplankton populations at 44 sites in Mobile Bay from December 2004, through June 2006, and at 5 sites in the Mississippi Sound from July 2005 through June 2006. These sites encompassed the major hydrological regimes in Mobile Bay and its adjacent waters in the Mississippi Sound. The data set used in describing these relationships consisted of sampling stations ranging spatially from the north end of MB to Horn Island and Biloxi Bay in the eastern MS, and temporally over an 18 month period. This temporal period encompassed a complete annual seasonal cycle, and included the excess nutrient flows, drought, and environmental changes occurring due to the passages of Hurricane Katrina and Hurricane Rita during the months of August and September, 2005. In this study it is shown that salinity, total nitrogen, and total phosphorous are the most significant factors driving phytoplankton populations in this region. It is inferred that the combined Mobile-Tensaw and Biloxi-Pascagoula River discharge influences abiotic variables, which in turn

influence the composition of phytoplankton populations. Seasonal patterns are shown to exist, with diatoms and dinoflagellates exhibiting population peaks in the winter and spring months, and chlorophytes and cryptophytes peaking in the summer and fall months. These results have implications in future regional planning of MB and MS, allowing better understanding of relationships between waters in the region and how decisions made for one area may affect others.

Chapter III investigated the utility of satellite data in the formation of a model for predicting the presence of the domoic acid producing diatoms of the genus *Pseudo-nitzschia*. The model predicts the presence of water conditions allowing for the formation of *Pseudo-nitzschia* spp. blooms with an omission accuracy of 21%. It is computationally simple, uses satellite data input products that are provided without cost and obtained, processed, and extracted to usable form for model input with relative ease by imagery download from the NASA Ocean Color website. Also, the capacity exists for automation by computer programming, and adjustment for accuracy with changing environmental conditions if different regions of the collection territory need to be monitored. Members of this genus are commonly represented, sometimes in high numbers ($<10^7$ cells L⁻¹), in phytoplankton collections undertaken by state health officials, fisheries management offices, and academic programs. The formation of this decision tree model allows a potential decision making tool to be made available for use by management officials to aid in the planning of collections and closure decisions.

Chapter IV provides algorithms allowing for regional prediction of salinity and CDOM through the use of SeaWiFS R_{rs} products at 510 nm and 555 nm. The algorithm uses the inherent relationships between CDOM and salinity. This relationship is based on

freshwater input and subsequent region specific riverine input of organic and inorganic nutrients, particularly DOC. Therefore the efficacy of the algorithm is tied to unique properties of water and specific to a particular body of water, such as the Mobile Bay discharge into the MS. The model uses input from both in situ collections of an Ocean Optics Spectroradiometer and SeaWiFS derived L_w and R_{rs} values of a 510 nm/555 nm wavelength ratio to predict CDOM, applying a second algorithm to predict salinity. A high predictive value was achieved ($R^2 = .91$) using simple linear equation applied to readily available satellite products.

In conclusion, this study showed that remote sensing does have utility toward the efforts to monitor and predict location of phytoplankton blooms in the Case II waters of the northern GoM. The characterization of phytoplankton populations in the MS and MB and the understanding of the relationship between salinity, surface temperature, and species composition has allowed for the formation of a decision tree model that is driven completely by satellite data. This model provides another tool for potential use by managers to enhance decision making processes for phytoplankton monitoring networks in the region. Owing to the relationships between salinity and phytoplankton populations noted in Chapter I, and the use of SeaWiFS derived data products as input values to the decision tree developed in Chapter II, the development of predictive algorithms for salinity will enhance the prediction of phytoplankton populations through allowing an input parameter not available through present satellite data collections.

APPENDIX
SPECIES LIST

Class level identification was achieved for 9 of 13 class level taxa. Diatoms (including the Bacillariophyceae, Fragilariophyceae, and Coscinodiscophyceae) were identified to genus. Dinoflagellates were identified to genus and species when possible, and to genus when identification to species was not possible, with light microscopy. A total of 41 genera of diatoms and 27 genera of dinoflagellates with representatives of >67 species of dinoflagellates were recorded during the study.

Class Level Taxa

Chlorophyceae
Prasinophyceae
Euglenophyceae
Chrysophyceae
Cryptophyceae
Bacillariophyceae
Fragilariophyceae
Coscinodiscophyceae
Dinophyceae
Dictyophyceae
Raphidophyceae

Diatom

Genera

Bacillaria
Bacteriastrum
Cylindrotheca
Cymbella
Diploneis
Gyrosigma
Haslea
Hemiaulus
Navicula
Nitzschia
Pleurosigma
Pseudo-nitzschia

Actinoptychus
Chaetoceros
Coscinodiscus
Cyclotella
Dactylosolen
Ditylum
Eucampia
Guinardia
Leptocylindrus
Lithodesmium
Melosira
Odontella
Paralia
Pseudoguinardia
Rhizosolenia
Proboscia
Pseudosolenia
Skeletonema
Stephanopyxis
Thalassiosira
Asterionella
Asterionellopsis
Cymatosira
Fragilaria
Lioloma
Rhaphoneis
Striatella
Synedra
Tabellaria
Thalassionema

Dinoflagellate
Genera/species

Akashiwo sanguinea
Amphidinium carterae
Amphidinium rotundata
Amphidiniopsis kofoidii
Ceratium furca
Ceratium fusus
Ceratium hircus
Ceratium lineatum
Ceratium trichoceros
Ceratium tripos
Cochlodinium sp.
Dinophysis acuta
Dinophysis acuminata

Dinophysis caudata
Dinophysis sp.
Diplopsalis lenticula
Gonyaulax digitale
Gonyaulax minima
Gonyaulax polygramma
Gonyaulax spinifera
Gonyaulax sp.
Gyrodinium estuariale
Gyrodinium simplex
Gyrodinium spirale
Heterocapsa rotundata
Heterocapsa sp.
Heterocapsa triquetra
Karenia brevis
Karenia mikimotoi
Karenia sp.
Karlodinium veneficum
Katodinium glaucum
Kryptoperidinium foliaceum
Lingulodinium sp.
Noctiluca scintillans
Oxyphysis oxytoxoides
Oxytoxum scolopax
Paleophalacroma sp.
Pheopolykrikos hartmannii
Podolampas palmipes
Polykrikos kofoidii
Polykrikos schwartzii
Prorocentrum compressum
Prorocentrum conicum
Prorocentrum emarginatum
Prorocentrum gracile
Prorocentrum mexicanum
Prorocentrum micans
Prorocentrum minimum
Prorocentrum scutellum
Prorocentrum triestinum
Prorocentrum sp.
Protoperidinium conicum
Protoperidinium crassipes
Protoperidinium depressum
Protoperidinium divergens
Protoperidinium grande
Protoperidinium leonis
Protoperidinium oblongum

Protoperidinium pellucidum
Protoperidinium pentagonum
Protoperidinium quinquecorne
Protoperidinium steidingerae
Protoperidinium sp.
Pyrophacus horologium
Scripsiella trochoidea

REFERENCES

- Anderson, D.M., Glibert, P.M., & Burkholder, J.M. (2002). Harmful algal blooms and eutrophication: nutrient sources, composition, and consequences. *Estuaries*, 25(4b), 704–726.
- Anderson, D. M., Burkholder, J. M., Cochlan, W. P., Glibert, P. M., Gobler, C. J., & Heil, C. A. (2008). Harmful algal blooms and eutrophication: Examining linkages from selected coastal regions of the United States. *Harmful Algae*, 8(1), 39-53.
- Antoine, D., Andre, J. M., & Morel, A. (1996). Oceanic primary production. Estimation at global scale from satellite (coastal zone color scanner) chlorophyll. *Global Biogeochemical Cycles*, 10, 57-69.
- Bargu, S., Powell, C.L., Coale, S.L., Busman, M., Doucette, G.J., & Silver, M.W. (2002). Krill: A potential vector for domoic acid in marine food webs. *Marine Ecology Progress Series*, 237, 209–216.
- Bates, S. S., Garrison, D. L., & Horner, R. (1998). Bloom dynamics and physiology of domoic-acid-producing *Pseudo-nitzschia* spp. In Anderson, D.M., Cembella, A.D., & Hallegraeff, G.M. (Eds.), *Physiological ecology of harmful algal blooms*, (pp. 267-292). Heidelberg, Germany: Springer-Verlag.
- Bates, S. S., & Trainer, V. L. 2006. The economic effects of harmful algal blooms. In *Ecology of Harmful Algae, Ecological Studies: analysis and synthesis*, 189. (pp. 81-93). (Eds.), Graneli, E., and Turner, J. Dordrecht, The Netherlands: Springer-Verlag.
- Bates, S. S., Bird, C. J., de Freitas, A. S. W., Foxall, R., Gilgan, M., Hanic, L. A., et al. (1989). Pennate diatom *Pseudo-nitzschia pungens* as the primary source of domoic acid, a toxin in shellfish from eastern Prince Edward Island, Canada. *Canadian*

Journal of Fish and Aquatic Science, 46, 1203-1215.

- Baya, E. E., Yokel, L. S., Pinyerd, C. A., Blancher, E. C., Sklenar, S. A., & Isphording, W. C. (1998). *Preliminary characterization of water quality of the Mobile Bay National Estuary Program study site*. Fairhope, AL, Mobile Bay National Estuary Program.
- Bledsoe, E., & Phlips, E. J. (2000). Relationships between phytoplankton standing crop and physical, chemical, and biological gradients in the Suwannee River and plume region, U.S.A. *Estuaries and Coasts*, 23(4), 458-473.
- Borak, J. S., & Strahler, A. H. (1999). Feature selection and land cover classification of a MODIS-like data set for semi-arid environment. *International Journal of Remote Sensing*, 20, 919–938.
- Bricker, S., Longstaff, B., Dennison, W., Jones, A., Boicourt, K., Wicks, C., & Woerner, J. (Eds.). (2007). *Effects of nutrient enrichment in the Nation's Estuaries: a decade of change*. Silver Spring, MD: National Centers for Coastal Ocean Science.
- Burkholder, J. M., Gustaaf M., Hallegraeff, G. M., Cohen, A., Bowers, H. A., Oldach, D. W., Parrow, M. W., Sullivan, M. J., Zimba, P. V., Allen, E. H., Kinder, C. A., & Mallin, M. A. (2007). Phytoplankton and bacterial assemblages in ballast water of U.S. military ships as a function of port of origin, voyage time, and ocean exchange practices. *Harmful Algae*, 6(4), 486-518.
- Cannizzaro, J. P., Hu, C., English, D. C., Carder, K. L., Heil, C. A., & Müller-Karger, F. E. (2009). Detection of *Karenia brevis* blooms on the west Florida shelf using in situ backscattering and fluorescence data. *Harmful Algae*, 8(6), 898-909.
- Carder, K. L., Chen, F. R., Lee, Z. P., Hawes, S. K., & Kamykowski, D. (1999).

Semianalytic moderate-resolution imaging spectrometer algorithm for chlorophyll-a and absorption with bio-optical domains based on nitrate-depletion temperatures.

Journal of Geophysical Research, 104, 5403–5421.

Clarke, K. R. (1993). Non-parametric multivariate analyses of changes in community structure. *Australian Journal of Ecology* 18, 117-143.

Clarke, K.R., & Warwicke, R.M. (2001). *Change in marine communities: An approach to statistical analysis and interpretation*. Plymouth, England:PRIMER-E.

Cloern, J. E. (1991). Tidal stirring and phytoplankton bloom dynamics in an estuary.

Journal of Marine Research, 49,203-221

Cortes-Altamirano, R., Hernandez-Becerril, D.U., & Luna-Soria, R. (1995). Mareas rojas en Mexico: Una revision. *Revista Latino Americana Microbiologia*, 37, 343-352.

Cowan, J. L. W., Pennock, J. R., & Boynton, W. R. (1996). Seasonal and inter-annual patterns of sediment-water nutrient and oxygen fluxes in Mobile Bay, Alabama (USA): Regulating factors and ecological significance. *Marine Ecological Progress Series*, 141, 229-245.

DeFries, R., & Townshend, J. R. G. (1994). Global land cover: Comparison of ground-based data sets to classifications with AVHRR data. In G. Foody & P. Curran (Eds.), *Environmental remote sensing from regional to global scales* (pp. 84-110). New York: John Wiley and Sons.

Del Castillo, C. E. (2005). Remote sensing of colored dissolved organic matter in coastal environments. In R. M. Miller, C. E. Del Castillo, & B. McKee (Eds.), *Remote sensing of aquatic coastal environment* (pp.157-180). New York: Springer.

Del Castillo, C. E., Coble, P. E., & Conmy, R. N. (2001). Multispectral in-situ

- measurements of organic matter and chlorophyll fluorescence in seawater:
documenting the intrusion of the Mississippi River plume in the West Florida Shelf.
Limnology and Oceanography, 46(7), 1836–1843.
- Del Castillo, C. E., Coble, P. G., Morel, J. M., Lopez, J. M., & Corredor, J. E. (1999).
Analysis of the optical properties of the Orinoco River Plume by absorption and
fluorescence spectroscopy. *Marine Chemistry*, 66, 35–51.
- Del Castillo, C. E., Gilbes, F., Coble, P. G., & Müller-Karger, F. E. (2000). On the
dispersal of riverine colored dissolved organic matter over the West Florida Shelf.
Limnology and Oceanography, 45(6), 1425–1432.
- Del Castillo, C.E. & Miller, R.L. (2008). On the use of ocean color remote sensing to
measure the transport of dissolved organic carbon by the Mississippi River Plume.
Remote Sensing of Environment, 11, 836-444.
- Del Vecchio, R., & Blough, N. V. (2002). Photobleaching of chromophoric dissolved
organic matter in natural waters: kinetics and modeling. *Marine Chemistry*, 78,
231–253.
- D'Sa, E. J., & Miller, R. L. (2003). Bio-optical properties in waters influenced by the
Mississippi River during low flow conditions. *Remote Sensing Environment*, 84(4),
538–549.
- D'Sa, E. J., Miller, R. L., & Del Castillo, C. E. (2006). An Assessment of short term
physical influences on the bio-optical properties and ocean color algorithms in coastal
waters influenced by the Mississippi River. *Applied Optics*, 45(28), 7410–7428.
- Dinnel, S. P., & Schroeder, W. W. (1989). Coastal water level measurements, northeast
Gulf of Mexico. *Journal of Coastal Research*, 5(3), 553-561.

- Dortch, Q., Robichaux, R., Pool, S., Milsted, D., Mire, G., Rabalais, N.N., Soniat, T.M., Fryxell, G.A., Turner, R.E., & Parsons, M.L. (1997). Abundance and vertical flux of *Pseudo-nitzschia* in the northern Gulf of Mexico. *Marine Ecological Progress Series*, 146 (1–3), 249–264.
- Engle, V. D., Kurtz, J. C., Smith, L. M., Chancy, C., & Bourgeois, P. (2007). A classification of U.S. estuaries based on physical and hydrologic attributes. *Environmental Monitoring Assessment*, 129(1-3), 397-412.
- Ferreira, S. B. & Simas, T. (2005). An integrated methodology for assessment of estuarine trophic status. *Ecological Modeling*, 169, 39–60.
- Field, J. G., Clarke, K. R., & Warwick, R. M. (1982). A Practical Strategy for Analysing Multispecies Distribution Patterns. *Marine Ecology Progress Series*, 8, 37-52.
- Gahegan, M. & West, G. (1998). The classification of complex data sets: An operational comparison of artificial neural networks and decision tree classifiers. In *Proceedings of the 3rd international conference on geocomputation, University of Bristol, UK, 17–19 September 1998*. University of Bristol, England.
- Gallegos, L., & Platt, T. (1982). Phytoplankton production and water motion in surface mixed layers. *Deep Sea Research Part A: Oceanographic Research Papers*, 29(1), 65-76.
- Garver, S., & Siegel, D. (1997). Inherent optical property inversion of ocean color spectra and its biogeochemical interpretation: time 1 series from the Sargasso Sea. *Journal of Geophysical Research*, 102C, 18607–18625.
- Gordon, H. R. (1995). Remote sensing of ocean color: A methodology for dealing with broad spectral bands and significant out-of-band response. *Applied Optics*, 34,

8363–8374.

- Gordon, H. R. (1997). Atmospheric correction of ocean color imagery in the Earth observing system era. *Journal of Geophysical Research*, D, 102, 17,081–17,106.
- Gordon, H. R., Brown, O. B., Evans, R. H., Brown, J. W., Smith, R. C., & Baker, K. S. (1988). A semi-analytic radiance model of ocean color. *Journal of Geophysical Research*, 93(D9), 10,909–10,924.
- Gordon, H. R., Clark, D. K., Mueller, J. L., & Hovis, W. A. (1980). Phytoplankton pigments derived from the Nimbus-7 CZCS: Initial comparisons with surface measurements. *Science*, 210, 63–66.
- Gordon, H. R., & Franz, B. A. (2008). Remote sensing of ocean color: Assessment of the water-leaving radiance bidirectional effects on the atmospheric diffuse transmittance for SeaWiFS and MODIS intercomparisons. *Remote Sensing of Environment*, 112(5), 2677-2685.
- Graneli, E., & Turner, J. T. (2006). An introduction to harmful algae. In E. Graneli & J. T. Turner (Eds.), *Ecology of Harmful Algae, Ecological Studies: analysis and synthesis*, 189, (pp. 391-402). The Netherlands: Springer-Verlag.
- Green, R. E., Gould, R. W., & Ko, D. S. (2008). Statistical models for sediment/detritus and dissolved absorption coefficients in coastal waters of the northern Gulf of Mexico. *Continental Shelf Research*, 28(10), 1273-1285.
- Harding, L., Itsweire, E. & Esaias, W., (1994). Estimates of phytoplankton biomass in the Chesapeake Bay from aircraft remote sensing of chlorophyll concentrations, 1989–92. *Remote Sensing of Environment*, 49, 41–56.
- Harding, L. W., Magnuson, A., & Mallonee, M. E. (2005). SeaWiFS retrievals of

chlorophyll in Chesapeake Bay and the mid-Atlantic bight. *Estuarine, Coastal and Shelf Science*, 62, 75–94.

HARRNESS (2005). Harmful algal research and response: A national environmental science strategy 2005–2015. Ramsdell, J.S., D.M. Anderson and P.M. Glibert (Eds.), Ecological Society of America, Washington DC, 96 pp.

Hasle, G. R. (2002). Are most of the domoic acid-producing species of the diatom genus *Pseudo-nitzschia* cosmopolites? *Harmful Algae*, 1(2), 137.

Hoagland, P., & Scatasta, S. (2006). The economic effects of harmful algal blooms. In E. Graneli & J. Turner (Eds.), *Ecology of Harmful Algae, Ecological Studies: analysis and synthesis*, 189, (pp. 391-402). The Netherlands: Springer-Verlag.

Hoge, F. E., Williams, M. E., Swift, R. N., Yungel, J. K., & Vodacek, A. (1995). Satellite retrieval of the absorption coefficient of chromophoric dissolved organic matter in continental margins. *Journal of Geophysical Research*, 100(28) 847-28,854.

Hoge, F. E., Wright, C. W., Lyon, P. E., Swift, R. N., & Yungel, J. K. (2001). Inherent optical properties imagery of the western North Atlantic Ocean: horizontal spatial variability of the upper mixed layer. *Journal of Geophysical Research*, 106(31), 129-31,140.

Hooker, S. B., & McClain, C. R. (2000). The calibration and validation of SeaWiFS data. *Progress In Oceanography*, 45(3-4), 427-465.

IOCCG (2000). Remote sensing of ocean colour in coastal, and other optically-complex, waters. S. Sathyendranath (Ed.), *Reports of the International Ocean Colour Coordinating Group*, No. 3, IOCCG, Dartmouth, Canada.

Isphording, W. C., & Lamb, G. M. (1979). *The sediments of Mobile Bay*. Dauphin Island

Sea Lab, Alabama Technical Report No. 80-002.

Jewett, E.B., Lopez, C.B., Dortch, Q., & Etheridge, S.M. (2007). National Assessment of Efforts to Predict and Respond to Harmful Algal Blooms in U.S. Waters. Interim Report. Interagency Working Group on Harmful Algal Blooms, Hypoxia, and Human Health of the Joint Subcommittee on Ocean Science and Technology. Washington, DC.

Johannessen, S.C., Miller, W.L., & Cullen, J.J.. (1999, January). An estimate of the marine photochemical source of dissolved inorganic carbon from SeaWiFS Ocean Colour. *Eos, Transactions of the American Geophysical Union*, 80: OS128, Abstract #OS22M-02 (2000 AGU-ASLO Ocean Sciences Meeting) San Antonio, TX.

Johnson, R.. (1978). Mapping of Chlorophyll a distribution in coastal zones.

Photogrammetric Engineering and Remote Sensing, 44, 617–624.

Kin-Chung, H., & Hodgkiss, I.J. (1991). Red tides in subtropical waters: an overview of their occurrence. *Asian Marine Biology*, 89, 5-23.

Kruskal, J. B. (1964). Multidimensional scaling by optimizing goodness of fit to a nonmetric hypothesis. *Psychometrika*, 29, 1-27.

Kuchinke, C. P., Gordon, H. R., Harding, L.W., Jr., & Voss, K. J. (2009). Spectral optimization for constituent retrieval in Case 2 waters II: Validation study in the Chesapeake Bay. *Remote Sensing of Environment*, 113, 610–621.

Landsberg, J. H. (2002). The effects of harmful algal blooms on aquatic organisms. *Reviews in Fisheries Science*, 10(2), 113-390.

Lanerolle, L. W. J., Tomlinson, M. C., Gross, T. F., Aikman Iii, F., Stumpf, R. P., & Kirkpatrick, G. J. (2006). Numerical investigation of the effects of upwelling on

- harmful algal blooms off the west Florida coast. *Estuarine, Coastal and Shelf Science*, 70(4), 599-612.
- Lehrter, J., Pennock, J., & McManus, G. (1999). Microzooplankton grazing and nitrogen excretion across a surface estuarine-coastal interface. *Estuaries and Coasts*, 22(1), 113-125.
- Lehrter, J. C. (2008). Regulation of eutrophication susceptibility in oligohaline regions of a northern Gulf of Mexico estuary, Mobile Bay, Alabama. *Marine Pollution Bulletin*, 56(8), 1446-1460.
- Levin, S. A. (1992). The problem of pattern and scale in ecology. *Ecology*, 73, 1943-1967.
- Liefer, J. D., MacIntyre, H. L., Novoveská, L., Smith, W. L., & Dorsey, C. P. (2009). Temporal and spatial variability in *Pseudo-nitzschia* spp. in Alabama coastal waters: A "hot spot" linked to submarine groundwater discharge? *Harmful Algae*, 8(5), 706-714.
- Lohrenz, S. E., Redalje, D. G., Verity, P. G., Flagg, C. N. & Matulewski, K. V. (2002). Carbon cycling and biogeochemistry in the northwest atlantic shelf slope: Results of the ocean margins program. *Deep Sea Research Part II*, 49(20), 4479-4509.
- Lohrenz, S. E., Fahnenstiel, G. L., Redalje, D. G., Lang, G. A., Dagg, M. J. & Whitedge, T. E. (1999). Nutrients, irradiance, and mixing as factors regulating primary production in coastal waters impacted by the Mississippi River plume. *Continental Shelf Research*, 19(9), 1113-1141.
- Loyacano, A., & Smith, J. P., (1979). An introduction to the waters of Mobile Bay, p. 1-7. In H. A. Loyacano, Jr. & J. P. Smith (Eds.), *Symposium on the National Resources*

- of the Mobile Estuary, Alabama* (pp. 1-7). U.S. Army Corps of Engineers, Mobile District, Mobile, Alabama.
- Lucas, L. V., Koseff, J. R., Cloern, J. E., Monismith, S. G., & Thompson, J. K. (1999a). Processes governing phytoplankton blooms in estuaries. I: The local production-loss balance. *Marine Ecology Progress Series*, 187, 1-15.
- Lucas, L. V., Koseff, J. R., Monismith, S. G., Cloern, J. E., & Thompson, J. K. (1999b). Processes governing phytoplankton blooms in estuaries. II: The role of horizontal transport. *Marine Ecology Progress Series*, 187, 17-30.
- Marshall, H. G., Lacouture, V., & Johnson, J. M. (2006). Phytoplankton assemblages associated with water quality and salinity regions in Chesapeake Bay, USA. *Estuarine, Coastal and Shelf Science*, 69(1-2), 10-18.
- Magaña, H. A., Contreras, C., & Villareal, T. A. (2003). A historical assessment of *Karenia brevis* in the western Gulf of Mexico. *Harmful Algae*, 2(3), 163-171.
- Maier Brown, A. F., Dortch, Q., Dolah, F. M. V., Leighfield, T. A., Morrison, W., & Thessen, A. E. (2006). Effect of salinity on the distribution, growth, and toxicity of *Karenia* spp. *Harmful Algae*, 5(2), 199-212.
- McClain, C. R., Feldman, G. C., & Hooker, S. B. (2004). An overview of the SeaWiFS strategies for producing a climate research quality global ocean bio-optical time series. *Deep-Sea Research II*, 51, 5-42.
- McClain, C. R., John, H. S., Karl, K. T., & Steve, A. T. (2009). Satellite Remote Sensing: Ocean Color. In J. Turner, S. Thorpe, & K. Turekian (Eds). *Encyclopedia of ocean sciences* (pp. 4403-4416). Oxford: Academic Press.
- Mobley, C. D. (1994). *Light and water: radiative transfer in natural waters*. San Diego:

Academic Press.

- Mobley, C. D. (1999). Estimation of the remote-sensing reflectance from above-surface measurements. *Applied Optics*, *38*, 7442–7455.
- Morel, A., & Gentili, B. (1991). Diffuse reflectance of oceanic waters: its dependence on sun angle as influenced by the molecular scattering contribution. *Applied Optics*, *30*, 4427–4438.
- Morel, A., & Gentili, B. (1996). Diffuse reflectance of oceanic waters: III. Implication of bidirectionality for the remote-sensing problem. *Applied Optics*, *35*, 4850–4862.
- Morel, A., & Gordon, H. R. (1980). Report of the working group on water color. *Boundary Layer Meteorology*, *18*, 343–355.
- Morel, A., & Prieur, L. (1977). Analysis of variations in ocean color. *Limnology and Oceanography*, *22*(4), 709–722.
- Mueller, J. L., & Austin, R. W. (1995). Ocean optics protocols for SeaWiFS validation, revision 1. NASA Technological Memo Number 104566, Vol. 25, SeaWiFS Technology Report Series.
- Murrell, M., Stanley, R., Lores, E., Didonato, G., Smith, L., & Flemer, D., (2002). Evidence that phosphorus limits phytoplankton growth in a Gulf of Mexico estuary: Pensacola Bay, Florida, USA. *Bulletin of Marine Science*, *70*, 155–167.
- Muylaert, K., Sabbe, K., & Vyverman, W. (2009). Changes in phytoplankton diversity and community composition along the salinity gradient of the Schelde estuary (Belgium/The Netherlands). *Estuarine, Coastal and Shelf Science*, *82*(2), 335–340.
- Nielsen, S. L., Sand-Jensen, K., Borum, J., & Geertz-Hansen, O. (2002). Phytoplankton, nutrients, and transparency in Danish coastal waters. *Estuaries*, *25*(5), 930–937.

- Noble, M. A., Schroeder, W. W., Wiseman, W. W., Ryan, H. F., & Gelfenbaum, G. R. (1997). Subtidal circulation patterns in a shallow, highly-stratified estuary: Mobile Bay, Alabama. *Journal of Geophysical Research*, *101*(11), 25689-25704.
- O'Reilly, J. E., Maritorena, S., Mitchell, B. G., Siegel, D. A., Carder, K. L., Garver, S. A., Kahru, M., & McClain, C. R. (1998). Ocean color chlorophyll algorithms for SeaWiFS. *Journal of Geophysical Research*, *103*, 24937–24953.
- Pal, M., & Mather, P. M. (2003). An assessment of the effectiveness of decision tree methods for land cover classification. *Remote Sensing of Environment*, *86*(4), 554-565.
- Park, K., Kim, C.-K., & Schroeder, W. W. (2007). Temporal variability in summertime bottom hypoxia in shallow areas of Mobile Bay, Alabama. *Estuaries and Coasts*, *30*(1), 54-65.
- Parsons, M. L., Dortch, Q., & Turner, R. E. (2002). Sedimentological evidence of an increase in *Pseudo-nitzschia* (Bacillariophyceae) abundance in response to coastal eutrophication. *Limnology and Oceanography*, *47*, 551-558.
- Pennock, J. R., Cowan, Jr., J. H., Shotts, K. M., Cowan, W., & Gallagher, L. J. (2001). *Weeks Bay data report WBAY-2 to WBAY-56 Cruises (May 1996 - May 2000)*. Dauphin Island, AL: Dauphin Island Sea Lab.
- Pennock, J. R., Schroeder, W. W., Lehrter, J. C., J. Cowan, L. W., & Blythe, F. (2002). *Mobile Bay data report MB-35 to MB-58 Cruises (July 1993 - August 1995)*. Dauphin Island, AL: Dauphin Island Sea Lab.
- Phlips, E. J., Badylak, S., & Grosskopf, T. (2002). Factors affecting the abundance of phytoplankton in a restricted subtropical lagoon, the Indian River Lagoon, Florida,

- USA. *Estuarine, Coastal and Shelf Science*, 55(3), 385-402.
- Phlips, E. J., Badylak, S., Youn, S., & Kelley, K. (2004). The occurrence of potentially toxic dinoflagellates and diatoms in a subtropical lagoon, the Indian River Lagoon, Florida, USA. *Harmful Algae*, 3(1), 39-49.
- Quinlan, E. L., & Phlips, E. J. (2007). Phytoplankton assemblages across the marine to low-salinity transition zone in a blackwater dominated estuary. *Journal of Plankton Research*, 29(5), 401-401.
- Rabalais, N. N., Dagg, M. J., & Boesch, D. F. (1985). Nationwide review of oxygen depletion and eutrophication in estuarine and coastal waters: Gulf of Mexico (Alabama, Mississippi, Louisiana, and Texas). Final Report to NOAA Ocean Assessment Division, Louisiana Universities Marine Consortium, Chauvin, Louisiana.
- Ransibrahmanakul, V. & Stumpf, R. P. (2006). Correcting ocean colour reflectance for absorbing aerosols. *International Journal of Remote Sensing*, 27, 1759 – 1774.
- Ryan, H. F., M., Noble, A., Williams, E. A., Schroeder, W. W., Pennock, J. R., & Gelfenbaum, G. (1997). Tidal current shear in a broad, shallow, river-dominated estuary. *Continental Shelf Research*, 17, 665–688.
- Schroeder, W. W. (1977). The impact of the 1973 flooding of the Mobile River system on the hydrography of Mobile Bay and east Mississippi Sound. *Northeast Gulf Science*, 1, 68-76.
- Schroeder, W. W. (1979). The dissolved oxygen puzzle of the Mobile Estuary. In H. A. Loyacano, & J. P. Smith (Eds.), *Symposium on the National Resources of the Mobile Estuary, Alabama*. Mobile, Alabama: U.S. Army Corps of Engineers,

Mobile District.

- Schroeder, W. W., Cowan, J. L. W., Pennock, J. R., Luker, S. A., & Wiseman, W. J., Jr. (1998). Response of resource excavations in Mobile Bay, Alabama, to extreme forcing. *Estuaries*, 21(4), 652-657.
- Schroeder, W. W., Dinnel, S. P., & Wiseman, W. J., Jr. (1990). Salinity stratification in a river-dominated estuary. *Estuaries*, 13(2), 145-154.
- Schroeder, W. W., Dinnel, S.P., & Wiseman, W. J., Jr. (1992). Salinity structure of a shallow, tributary estuary, p. 155–171. In D. Prandle (Ed.), *Dynamics and Exchanges in Estuaries and the Coastal Zone, Coastal and Estuarine Studies 40*. Washington, D.C.: American Geophysical Union.
- Schroeder, W. W. & Wiseman, W. J., Jr. (1986). The Mobile Bay estuary: Stratification, oxygen depletion, and jubilees. In B. Kjerfve (Ed.), *Hydrodynamics of estuaries, Volume II, Estuarine case studies* (pp. 41-52). Boca Raton: CRC Press.
- Siegel, D. A., Maritorena, S., Nelson, N. B., Behrenfeld, M. J., & McClain, C. R. (2005). Colored dissolved organic matter and its influence on the satellite based characterization of the ocean biosphere. *Geophysical Research Letters*, 32, 205-206.
- Smayda, T.J. (1990). Novel and nuisance phytoplankton blooms in the sea: Evidence for a global epidemic. In *Toxic Marine Phytoplankton*, (pp. 29-40). E. Granéli, B. Sundström, L. Edler, and D.M. Anderson, (Eds.), New York: Elsevier.
- Smayda, T.J. (1997). Harmful algal blooms: Their ecophysiology and general relevance to phytoplankton blooms in the sea. *Limnology and Oceanography* 42, 1137-1153.
- Solomatine, D.P., & Dulal, K.N. (2003). *Model tree as an alternative to neural network in rainfall-runoff modelling*, Hydrological Sciences Journal, 48(3), 399–411.

- Sommer, U. (1994). Are marine diatoms favored by high Si:N ratios? *Marine Ecological Progress Series*, 115 (3), 309–315.
- Stanley, D. W., & Nixon, S. W. (1992). Stratification and bottom water hypoxia in the Pamlico River estuary. *Estuaries*, 15:270–281.
- Steidinger, K.A., Landsberg, J.H., Truby, E.W., & Roberts, B.S. (1998) First report of *Gymnodinium pulchellum* (Dinophyceae) in North America and associated fish kills in the Indian River, Florida. *Journal of Phycology*, 34 (3): 431-437.
- Steidinger, K.A., & Penta, H.M., (Eds.) (1999). *Harmful microalgae and associated public health risks in the Gulf of Mexico*. In: EPA Gulf of Mexico Program Office.
- Stumpf, R. P., Culver, M. E., Tester, P. A., Tomlinson, M., Kirkpatrick, G. J., & Pederson, B. A. (2003). Monitoring *Karenia brevis* blooms in the Gulf of Mexico using satellite ocean color imagery and other data. *Harmful Algae*, 2(2), 147-160.
- Stumpf, R. P., & Pennock, J. R. (1991). Remote estimation of the diffuse attenuation coefficient in a moderately turbid estuary. *Remote Sensing of Environment*, 38, 183–191.
- Stumpf, R. P., Tomlinson, M. C., Calkins, J. A., Kirkpatrick, B., Fisher, K., & Nierenberg, K. (2009). Skill assessment for an operational algal bloom forecast system. *Journal of Marine Systems*, 76(1-2), 151-161.
- Tatem, A. J., Goetz, S. J., & Hay, I. (2004). Terra and Aqua: new data for epidemiology and public health. *International Journal of Applied Earth Observation and Geoinformation*, 6(1), 33-46.
- Thessen, A.E., Dortch, Q., Parsons, M.L., & Morrison, W. (2005). Effect of salinity on *Pseudo-nitzschia* species (Bacillariophyceae) growth and distribution. *Journal of*

- Phycology*, 41(1), 21-29.
- Thomann, R. V., & Mueller, J. A. (1987). *Principles of surface water quality modeling and control*. New York: Harper and Row.
- Tomlinson, M. C., Stumpf, R. P., Ransibrahmanakul, V., Truby, E. W., Kirkpatrick, G. J., Pederson, B. A. (2004). Evaluation of the use of SeaWiFS imagery for detecting *Karenia brevis* harmful algal blooms in the eastern Gulf of Mexico. *Remote Sensing of Environment*, 91(3-4), 293-303.
- Trainer, V.L., Adams, N.G., Bill, B.D., Stehr, C.M., Wekell, J.C., Moeller, P., Busman, M., & Woodruff, D. (2000). Domoic acid production near California coastal upwelling zones, June 1998. *Limnology and Oceanography*, 45(8), 1818–1833.
- Trainer, V. L., Hickey, B. M., & Horner, R. A. (2002). Biological and physical dynamics of domoic acid production off the Washington coast. *Limnology and Oceanography*. 47(5), 1438–1446.
- Turner, R. E., Schroeder, W. W., & Wiseman Jr., W. J. (1987). The role of stratification in the deoxygenation of Mobile Bay and adjacent shelf bottom waters. *Estuaries*, 10, 13–19.
- USEPA (1999). Ecological condition of estuaries in the Gulf of Mexico. EPA 620-R-98-004. U.S. Environmental Protection Agency, Office of Research and Development, National Health and Environmental Effects Research Laboratory, Gulf Ecology Division, Gulf Breeze, FL.
- Villareal, T.A., Brainard, M.A., & McEachron, L.W. (2001). *Gymnodinium breve* in the western Gulf of Mexico, resident versus advected populations as a seed stock for blooms. In: G. Hallegraeef, S.I. Blackburn, A., C.J. Bolch, & R.J. Lewis, (Eds.),

- Harmful Algal Blooms 2000. Intergovernmental Oceanographic Commission of UNESCO*, (pp. 153–156). Paris: UNESCO.
- Ward, G. M., Harris, P. M., Ward, A. K., Arthur, C. B., & Colbert, E. C. (2005). Gulf Coast rivers of the Southeastern United States. In A. Benke & C. Cushing (Eds.), *Rivers of North America*, (pp. 124-178). Burlington: Academic Press.
- Warwick, B. & Paul, J.H. 2004. Phytoplankton community structure and productivity along the axis of the Mississippi River plume in oligotrophic Gulf of Mexico waters. *Aquatic Microbial Ecology* 35, 185-196.
- West, B. J., Geneston, E. L., & Grigolini, P. (2008). Maximizing information exchange between complex networks. *Physics Reports*, 468(1-3), 1-99.
- West, D., & Dellana, S. (2009). Diversity of ability and cognitive style for group decision processes. *Information Sciences*, 179(5), 542-558.
- Wilber, D. H., Clarke, D. G., & Rees, S. I. (2007). Responses of benthic macroinvertebrates to thin-layer disposal of dredged material in Mississippi Sound, USA. *Marine Pollution Bulletin*, 54(1), 42-52.
- William, S., Jean, C., Jonathan, P., Steve, L., & William, W. (1998). Response of resource excavations in Mobile Bay, Alabama, to extreme forcing. *Estuaries and Coasts*, 21(4), 652-657.
- William, S., Jean, C., Jonathan, P., Steve, L., & William, W. (1998). Response of resource excavations in Mobile Bay, Alabama, to extreme forcing. *Estuaries and Coasts*, 21(4), 652-657.